

THE UNIVERSITY OF HULL

**Synthesis of new calixarene-based  
scandium precursors for medical  
imaging**

Being a Thesis submitted for the Degree of

Master of Science by Research

at the University of Hull

December 2018

By

MOHAMMED ABDULHADI R. ALAMRI

BSc. from KAU. 2009

Master. from USyd. 2015

This copy of the thesis has been supplied on condition that anyone who consults it is understood to recognise that its copyright rests with the author and that no quotation from this thesis, nor any information derived therefrom, may be published without the author's prior, written consent.

## Abstract

Targeted radionuclide therapy is a new and an effective approach for cancer imaging and therapy complementary to the existing methods. In the last decade, the use of metal complexes in imaging and therapy has gained commonality in most clinical situations. The development of  $^{99m}\text{Tc}$  radiopharmaceuticals initiated the coordination chemistry studies as it relates to diagnostic imaging. Currently, there are many types of radio metal complexes used in PET and gamma scintigraphy.

Scandium, of all the emitters, is an innovative element for Nuclear Medicine and has attracted attention as a prospective radionuclide for PET imaging. It has an isotope appropriate for targeted radionuclide therapy (Scandium 47) as well as for imaging by PET (Scandium 44). Lately, scandium isotopes ( $^{47}\text{Sc}$ ,  $^{44}\text{Sc}$ ) are readily obtainable and their qualities are suitable for PET imaging or radiotherapy.

Furthermore, Calixarenes have the capacity to complex a variety of molecules in aqueous phase, which is fascinating for biological application. The facile functionalization of calixarenes at the lower or upper rim, allows for readily adjustable properties, viz solubility, emission and biological recognition.

In this project, we tried to exploit the properties of both scandium and calixarenes and use the calixarenes as a scaffold to investigate their potential to transport a scandium radiolabel. We focused on the synthesis of new scandium calixarene complexes as precursors for medical imaging. We synthesised four new scandium-calixarene complexes.

## **Acknowledgement**

First, I thank God worthy of thanks and praise.

Second, I thank my supervisor Professor Carl Redshaw who guided me throughout this project and gave me all the time and support needed.

Third, I thank the government of Saudi Arabia for giving me every reason to advance and achieve my goals by the unlimited support they have given me including the sponsorship to this degree that was provided to me by Taif University.

Forth, I thank my second supervisor Dr. Timothy Prior who did most of the crystallography needed in this project. I also thank Dr. Mark Elsegood for crystallography work done on one of my complexes.

Fifth, I thank the University of Hull in which I did this research.

Sixth, I thank my parents, my wife and the rest of my family who will remain the reason behind any success that I achieved or may achieve.

Seventh, I thank my friends and colleagues Sultan Alqarni, Abdullah Alshamarani, Yahya Alkhafaji, David Miller, Tian Xing and Kuiyuan Wang for their help and for being great people to work with.

## List of Abbreviation

PET	Positron-emission tomography
MRI	Magnetic resonance imaging
SPECT	Single Photon Emission Computed Tomography
KeV	Kilo Electron Volt
MAb	Monoclonal antibodies
$t_{1/2}$	Half life
DOTA	1,4,7,10-Tetraazacyclododecane-1,4,7,10-tetraacetic acid
BAPTA	1,2-bis( <i>o</i> -aminophenoxy)ethane- <i>N,N</i> ,- <i>N',N'</i> -tetraacetic acid
DTPA	diethylenetriaminepentaacetic acid
TTHA	triethylenetetramine- <i>N,N,N',N'',N''',N''''</i> -hexaacetic acid
HBED	<i>N,N'</i> -di(2-hydroxybenzyl)ethylenediamine- <i>N,N'</i> - diacetic acid
EGTA	ethylenebis(oxyethylenedinitrilo)-tetraacetic acid
NMR	Nuclear Magnetic Resonance
IUPAC	International Union of Pure and Applied Chemistry
HPLC	High performance liquid chromatography
SLNs	SYBYL line notations
TB	Tuberculosis
HIV	Human Immunodeficiency Virus
PBS	Phosphate-buffered saline
MeCN	Acetonitrile
DMSO	Dimethyl sulfoxide
THF	Tetrahydrofuran
DCM	Dichloromethane

## List of figures

- Figure 1.1.** Folic acid conjugate with a DOTA
- Figure 1.2.** Structure of Połosak *et al.* ligands
- Figure 1.3.** Greek Calyx krater vase on the left and Calixarene on the right
- Figure 1.4.** Structure of calix[4]arene with carboxylic acid function at the phenolic end
- Figure 1.5.** Polyoxyethylene ether *p-tert-octylcalix[8]arene*
- Figure 1.6.** Structure of Coleman *et al.* compound that has the highest anticoagulant activity
- Figure 1.7.** The structures of anti-herpetic agents by Motornaya *et al*
- Figure 1.8.** Hamilton's most promising anti-viral agent
- Figure 1.9.** Antimicrobial calixarene derivatives reported by Casnati *et al*
- Figure 1.10.** Re-calixarene radiopharmaceutical precursor
- Figure 1.11.** Structure of calixarene derivative for Ac<sup>3+</sup> labelling
- Figure 1.12.** Examples of Redshaw *et al.* rhenium calixarene complexes
- Figure 1.13.** The structure of Redshaw's vanadyl calixarene complex.
- Figure 1.14.** The first X-ray structure of an oxa-calix[3]arene Sc complex
- Figure 1.15.** Structure of Webb, *et al.* scandium calix[4]arene complex in the absence of [18]crown-6.
- Figure 1.16.** Structure of Webb, *et al.* scandium calix[4]arene complex in the presence of [18]crown-6.
- Figure 1.17.** Structure of Gou, *et al.* scandium calix[6]arene complex.
- Figure 1.18.** Structure of Estler, *et al.* scandium calix[4]arene complex.
- Figure 2.1.** The chemical structures of the three ligands used in this work
- Figure 2.2.** View of molecular structure of complex **(1)**. The hydrogen atoms and the *t*Bu of calixarenes are removed for clarification
- Figure 2.3.** Alternative view of complex **(1)**. The hydrogen atoms and the *t*Bu of calixarenes are removed for clarification

- Figure 2.4.** A view of the core of complex **(1)**. calix[4]arenes are removed for clarification
- Figure 2.5.** View of molecular structure of complex **(2)**. The hydrogen atoms are removed for clarification
- Figure 2.6.** Molecular structure of complex **(2)**. Asymmetric unit with atoms drawn as 30% probability ellipsoids.
- Figure 2.7.** Alternative view of complex **(2)**. A single  $\text{Sc}_4\text{O}(\text{calix-4})_4$  cluster. For clarity, hydrogen atoms and *t*-butyl groups are not shown
- Figure 2.8.** Core of complex **(2)**. For clarity, only the Sc and O atoms are shown.
- Figure 2.9.** View of molecular structure of complex **(3)**. The hydrogen atoms are removed for clarification
- Figure 2.10.** Core of complex **(3)**. For clarity, only the Sc and O atoms are shown from two different view angles
- Figure 2.11.** View of molecular structure of complex **(4)**. The hydrogen atoms and the *t*Bu of calixarenes are removed for clarification
- Figure 2.12.** Alternative view of complex **(4)**. Hydrogen atoms and *t*-butyl groups of the calix[6]arenes are removed for clarification.
- Figure 2.13.** View of molecular structure of complex **(5)**. The hydrogen atoms and the *t*Bu of calixarenes are removed for clarification
- Figure 2.14.** The molecular structure of complex **(5)**. Hydrogen atoms are removed for clarification.

## List of tables

- Table 1.1.** Examples of anti-tumour calixarenes
- Table 1.2.** Calixarenes as a MRI contrast agents

## Contents

<b>Title</b>	<b>1</b>
<b>Abstract</b>	<b>2</b>
<b>Acknowledgement</b>	<b>3</b>
<b>List of Abbreviation</b>	<b>4</b>
<b>List of figures</b>	<b>5</b>
<b>List of tables</b>	<b>7</b>
<b>Chapter 1</b>	<b>10</b>
<b>Introduction</b>	<b>10</b>
<b>1.1. Cancer imaging</b>	<b>11</b>
<b>1.2. Radionuclides</b>	<b>13</b>
<b>1.3. Scandium</b>	<b>15</b>
1.3.1. Synthesis	17
<b>1.4. Calixarenes</b>	<b>22</b>
1.4.1. History	22
1.4.2. Synthesis	24
1.4.3. Properties	25
1.4.4. Chemical modification	26
1.4.4.1. Water-soluble calixarenes	26
1.4.4.1.1. Carboxylate functions	27
1.4.5. Biological activities	28
1.4.5.1. Toxicity of the calixarenes	29
1.4.5.2. Anti-tuberculosis calixarenes	30
1.4.5.3. Anti-thrombotic calixarenes	31
1.4.5.4. Anti-viral calixarenes	32
1.4.5.5. Anti-microbial calixarenes	34
1.4.5.6. Calixarenes as anti-cancer drugs	35
1.4.5.7. Calixarene in radiotherapy	40
1.4.5.8. Calixarenes as MRI contrast agents	44
<b>1.5. Known Scandium calixarenes</b>	<b>46</b>
<b>Chapter 2</b>	<b>50</b>
<b>Results and Discussion</b>	<b>50</b>
<b>2.1. Aims</b>	<b>51</b>
<b>2.2. <i>p</i>-tert-butylcalix[4]arene chemistry</b>	<b>52</b>
<b>2.3. <i>p</i>-tert-butylcalix[6]arene chemistry</b>	<b>59</b>
<b>2.4. <i>p</i>-tert-butylcalix[8]arene chemistry</b>	<b>63</b>
<b>2.5. Conclusion</b>	<b>65</b>
<b>Chapter 3</b>	<b>66</b>
<b>Experiment Section</b>	<b>66</b>
<b>3.1. General Consideration</b>	<b>67</b>
<b>3.2. Synthesis of (calix-4-H<sub>2</sub>)<sub>6</sub>Sc<sub>9</sub>(OH)<sub>8</sub>(MeCN)<sub>4</sub>·11MeCN (1).</b>	<b>68</b>

3.3. Synthesis of $[\text{Sc}_4\text{O}(\text{calix-4})_4] \cdot 12\text{C}_6\text{H}_5\text{CH}_3$ (2).	68
3.4. Synthesis of $[\text{Sc}_4\text{O}(\text{calix-6})_2]\text{C}_8\text{H}_{12}\text{N}_4\text{Na}0.5(\text{C}_6\text{H}_9\text{N}_3\text{Na}) \cdot 6\text{MeCN}$ (3).	69
3.5. Synthesis of $[(\text{calix-6})_2\text{Li}_4\text{Cl}(\text{THF})_2\text{BuOH}] \cdot \text{MeCN}$ (4).	69
3.6. Synthesis of $[\text{Sc}(\text{tBuCalix}[8]\text{areneH}_5)(\text{DMSO})_3] \cdot \frac{1}{2}\text{DMSO} \cdot 4\frac{1}{2}\text{MeCN}$ . (5).	70
<i>References</i>	71
<i>Appendix</i>	75

## **Chapter 1**

### **Introduction**

## 1.1. Cancer imaging

Cancer has become one of the research topics that many researchers across the globe have looked into. According to world health organisation, cancer is the second leading cause of death globally and about one in six deaths is due to cancer.<sup>1</sup> Currently, chemotherapy, surgery and external irradiation and radionuclide therapy, which is a new and an effective approach for cancer therapy complementary to the existing therapies.<sup>2</sup> The technique functions with a specific vector such as a peptide or an antibody. The radioactive isotope labels the vector and targets the cell to destroy.<sup>2</sup> Nuclear medicine provides both therapeutic drugs and diagnostic tools.<sup>3</sup> The commonly used imaging modalities in radiology are: (1) gamma scintigraphy (2) PET and, (3) MRI.

For Gamma scintigraphy, the following is required: a radiopharmaceutical containing nuclide (for emitting the gamma ( $\gamma$ ) radiation) and a gamma camera/single photon emission computed tomography (SPECT) camera that can image the individual who has been injected with gamma emitting radiopharmaceutical. In the case of PET, a PET camera capable of imaging the patient and radiopharmaceutical containing positron-emitting radionuclide ( $\beta$ ) is required. Positron decay functions by emitting of two 511 keV photons at 180° apart. Moreover, PET scanners have circular array of detectors whose core function is to detect the 511keV photons emitted in the opposite direction.

Metal complexes are used in both imaging modalities. However, Gamma scintigraphy is the most common and widely used imaging modality in most clinical situations.<sup>4</sup>

In clinical situations, with imaging modalities such as (gamma scintigraphy and PET), radiopharmaceuticals containing metal radionuclides are injected into a patient in order to diagnose problems such as cancer, cardiological disorders, neurological problems, kidney abnormalities and liver infections. The distribution of radiopharmaceuticals in the body depends on two factors; (1) through blood flow also referred as perfusion and (2) certain biological processes e.g. receptors, binding antigen.<sup>4</sup>

Recently, positron emission tomography has become powerful and the most applied imaging technology. Despite the similarities in the basic principles of PET and SPECT, PET is more sensitive than SPECT since it has a better spatial resolution and thus providing more accurate attenuation.<sup>5, 6</sup>

The continued development of targeted imaging agents for positron emission tomography (PET), relying on biomolecules and nanoparticles, stimulates research on radionuclide with a half-life matching their biological properties.<sup>7-9</sup> In radio imaging, the radioisotope applied should emit  $\gamma$  rays of suitable energy. For therapy, the radioisotopes used should decay by emitting  $\beta^-$  or  $\alpha$  particle. The particles emitted destroy the surrounding cells with respect to where they were delivered. The key challenge in this therapy is in delivering the radioisotopes to the targeted area and to compromise between toxicity to healthy tissues and anti-tumour effect. Therefore, these radioisotopes have to be selective and

bind to the target through a targeting vector. If the radioisotopes do not reach the targeted area, they should be eliminated from the patient's body while they are unchanged.<sup>3</sup>

## 1.2. Radionuclides

In the last decade, the use of metal complexes in imaging and therapy has gained commonality in most clinical situations. In addition, it has been a topic of research where many researchers across the globe have engaged. After the end of the World War II, nuclear technology was used for medical interventions and thus opening nuclear reactors for radioisotopes production. Iodine-131 ( $^{131}\text{I}$ ) was the very first radioisotope to be used and was used to treat thyroid cancer in 1946. More developments were seen in 1959 where the Brookhaven National Laboratory came up with the  $^{99}\text{Mo}:\text{}^{99\text{m}}\text{Tc}$  generator. In 1964, Argonne National Laboratory developed the first  $^{99\text{m}}\text{Tc}$  radiotracers. Today,  $^{99\text{m}}\text{Tc}$  is the mostly used radionuclide in diagnostic imaging. The development of  $^{99\text{m}}\text{Tc}$  radiopharmaceuticals began the study of coordination chemistry as it relates to diagnostic imaging. Currently, there are wide variety of radiometal complexes used in PET and gamma scintigraphy. The application of paramagnetic metal complexes is the most recent development, which is used for enhancing MRI (magnetic resonance imaging) contrast.<sup>4</sup>

During the designation of radio metal-based radiopharmaceuticals, it is of essence to be considerate of the following factors: the mode of decay of

the radioisotope, its half-life, availability as well as the cost of the radioisotope.

For medical imaging, most radionuclides decay by gamma emission since most clinical diagnostic imaging applies gamma scintigraphy as their modality.<sup>4</sup> In the case of PET, radionuclides decay by positron emission whereas in therapy, radionuclides emit alpha ( $\alpha$ ) or beta ( $\beta$ ) and many of them emits gamma ( $\gamma$ ) photons to be applied in both imaging and therapy. Gamma photons energy considered of essence since gamma cameras are designed for specific energy windows, generally in the range of 100–200 keV. Radionuclides that emits gamma photons of higher or lower energy than the mentioned; are likely not to be used in radio imaging. The half-life of the radioisotope should be long enough (this is to ensure that it carries out the desired chemistry to synthesize radiopharmaceutical) and should be short enough to limit the dose to the patient.<sup>4</sup> The half-life of the radiometals used in radiopharmaceuticals of gamma scintigraphy and PET ranges from 10 minutes ( $^{62}\text{Cu}$ ) to several days ( $^{67}\text{Ga}$ ). The required half-life is usually dependent on the time required for radiopharmaceuticals to localize in the target area. For instance, brain or heart radiopharmaceuticals require a short time (shorter half-life) because they reach the target faster. On the other hand, tumour targeted radiopharmaceutical requires a longer half-life to reach the localized target.<sup>4</sup>

Both metallic and non-metallic radioisotopes are used in medicine. The commonly used non-metallic isotopes include  $^{18}\text{F}$ ,  $^{13}\text{N}$ ,  $^{15}\text{O}$ , and  $^{131}\text{I}$ . On the other hand, metallic ones include  $^{99\text{m}}\text{Tc}$ , and most of the emerging

isotopes (e.g.,  $^{44}\text{Sc}$ ,  $^{68}\text{Ga}$ ,  $^{90}\text{Y}$ ,  $^{111}\text{In}$ ,  $^{153}\text{Sm}$ ,  $^{177}\text{Lu}$ , etc.). Ions of the metallic elements need to be tightly bound in complexes to avoid non-specific deposition of radiation, and the complexes must be eliminated from the body easily.<sup>3</sup> These complexes must be in a position to demonstrate high thermodynamic stability and kinetic inertness. Moreover, the ligands have to exhibit fast complexation of the metallic radioisotopes even in highly diluted solutions. They also must exhibit high selectivity for a particular metallic ion and have the ability to conjugate with biological vector molecules. Various literatures have indicated that it is a multidisciplinary field, which involves chemistry, physics, biology and medicine.<sup>10-16</sup>

### 1.3. Scandium

Scandium, of all the emitters observed in this category, is an innovative element for Nuclear Medicine and has attracted attention as a prospective radionuclide for PET imaging.<sup>17</sup> It has an isotope appropriate for targeted radionuclide therapy (Scandium 47) as well as for imaging by PET (Scandium 44).<sup>2</sup> Many benefits may be obtained from the use of  $^{44}\text{Sc}$  ( $t_{1/2} = 3.97$  h,  $E_{\text{mean}}(\beta^+) = 632$  keV, branching ratio = 94.3%). With a high positron fraction and almost four times the  $^{68}\text{Ga}$ 's half-life,  $^{44}\text{Sc}$  makes possible the production of an extensive selection of radiotracers with greater pharmacokinetic profiles while providing sufficient room for its posterior transfer to far-off PET facilities.<sup>18</sup>  $^{44}\text{Sc}$  was recently proposed as an alternative radionuclide for PET imaging by use of radio-metal peptides and other small-molecular-weight bio-molecules.<sup>17</sup>

Furthermore, the occurrence of  $^{47}\text{Sc}$  as an isotope with incredible prospect for radionuclide therapy, offers the chance for the use of  $^{44}\text{Sc}/^{47}\text{Sc}$  isotopic pair in assessment of therapeutic responses, disease diagnosis, therapy, and dosimetry estimation.<sup>19</sup> Lately, scandium isotopes ( $^{47}\text{Sc}$ ,  $^{44}\text{Sc}$ ) are readily obtainable and their qualities are suitable for PET imaging or radiotherapy. They can jointly be used in theranostic approach as “matched pair”.<sup>3</sup>

Current advancements show an apparent drift towards a patient-based personalized method of treating sickness, comprising of the accurate preparation and precise management of a particular therapeutic procedure for a specific patient.<sup>20</sup> This could be accomplished when a pair of isotopes, one for imaging and the other dedicated for treatment, is used.<sup>2</sup> Through imaging, the patient’s dosimetry and pharmacokinetics facts are acquired enabling for accurate tuning of the injection practice of the isotope for treatment. This can be executed by the use of similar compound labelled with a  $^{44}\text{Sc}$   $\beta^+$  emitter for PET images to be acquired and dosimetry can be evaluated before the combination with  $^{47}\text{Sc}$   $\beta^-$  emitter, to regulate the injected dosage to reduce toxicity and make best use of patient reaction. This is the fundamental standard of Theranostic Radiopharmaceuticals, which will lead to individualized treatment.<sup>21</sup>

$^{47}\text{Sc}$  possess a 3.35-day half-life, and displays a primary  $\gamma$ -ray at 159 keV, appropriate for planar and SPECT imaging.<sup>2</sup> Its physical properties are close to  $^{177}\text{Lu}$  or  $^{67}\text{Cu}$ , making it a suitable choice for targeted radionuclide therapy with correct properties.<sup>22</sup> The use of  $^{47}\text{Sc}$ , as a substitute radionuclide to  $^{177}\text{Lu}$ , was suggested in previous studies.<sup>23, 24</sup> As a trivalent

element, scandium ought to have similar properties to  $^{177}\text{Lu}$ .<sup>2</sup> In relation to  $^{177}\text{Lu}$ , the benefit of  $^{47}\text{Sc}$  production is the comparatively easy separation of the radionuclide from the target, while the drawback is the lesser cross-section of the nuclear reaction.<sup>25</sup> In addition, Scandium shows suitable chemistry for combination to monoclonal antibodies (MAb)-chelate systems.<sup>2</sup> It is similar in composition to  $^{90}\text{Y}$ , and the same ligands formed for  $^{90}\text{Y}$  can be applied in chelating  $^{47}\text{Sc}$ . In comparison to fluorine-18 or gallium-68, the extended half-life of  $^{44}\text{Sc}$  could tolerate the PET imaging of bigger antibody and peptides fragments that are presently restricted because of the short half-lives of normally applied PET radionuclide.<sup>2</sup>

### 1.3.1. Synthesis

There are two major methods for  $^{44}\text{Sc}$  synthesis: The capable PET isotope,  $^{44}\text{Sc}$ , can be easily synthesized by the  $^{44}\text{Ti}/^{44}\text{Sc}$  generator,<sup>26-28</sup> prevailing over the reliance on costly accelerators.<sup>7-9</sup> With its extended half-life of 59 years, the  $^{44}\text{Ti}$  can give a cyclotron-independent supply of  $^{44}\text{Sc}$  for several years.<sup>29, 30</sup> Various techniques were previously examined to build up the chemistry of  $^{44}\text{Ti}/^{44}\text{Sc}$  generators.<sup>31-33</sup> Filosofov *et al.* (2010) demonstrated an 185MBq (5 mCi) generator system with the appropriate radiochemical limits, for instance a low Breakthrough of  $< 5 \times 10^{-5} \%$  of  $^{44}\text{Ti}$  and  $>97\%$  elution efficiency for  $^{44}\text{Sc}$ .<sup>30</sup> This generator was also examined in the context of post-processing of the equation to facilitate the provision of high radiochemical purity and radionuclide concentration in batches of  $^{44}\text{Sc}$  in an aqueous system relevant to successive labelling results.  $^{44}\text{Ti}$  ( $t_{1/2} = 60 \text{ y}$ ), however, can just be produced at a limited number of premises in the globe, with small production and at lofty costs.<sup>34</sup> Severin *et*



The radio-Sc<sup>3+</sup> ion ought to be firmly bound for use in medicinal/biological applications.<sup>3</sup> Ligands appropriate for lanthanide(III) ions are supposed to be appropriate for Sc<sup>3+</sup> ion as well since scandium is a member of the rare earth metals; nevertheless, the chemistry of trivalent scandium is very complex.<sup>38-40</sup>

The <sup>44</sup>Sc seems to be suitable candidate in PET/CT analysis because of its physicochemical features of a trivalent exceptional earth metal. Used for radiopharmaceutical, macro-cyclic chelators are famous in building stable complexes with metal cations.<sup>41</sup> A small number of researches have, to date, demonstrated the production and execution of <sup>44</sup>Sc radiopharmaceutical for PET imaging, where a good number of them display only reserved achievement *in vivo*.<sup>42</sup>

Hernandez, *et al.* 2014,<sup>18</sup> stated the initial illustration of the production of a peptide-based radiotracer for PET imaging via cyclotron produced <sup>44</sup>Sc. in addition, they proved that <sup>44</sup>Sc extracted from the proton irradiation of unenriched Ca targets and separated using extraction chromatography gave an excellence element with great radionuclide purity and detailed activity, in an exceedingly cost-effective way. According to *in vivo* integrin  $\alpha_v\beta_3$  targeting assessment in a human glioblastoma animal model, <sup>44</sup>Sc is a feasible substitute to additional radiometals (e.g., <sup>68</sup>Ga and <sup>64</sup>Cu) for peptide-based PET.

Eigner, *et al.* 2012,<sup>43</sup> primarily demonstrated the positive PET imaging using <sup>44</sup>Sc extracted from a <sup>44</sup>Ti/<sup>44</sup>Sc generator. In two subcutaneous tumour representations [44Sc]-DOTA-Pur displayed big tumour-to-background ratios. The outcome mainly showed rapid blood clearance and renal excretion. Activity build up in the tumours attained an early limit. Tumour-to-muscle contrast was always positive. This work also demonstrated that maximization of the tracer to achieve extended tumour absorption and half-life in blood to enhance in vivo kinetics and developments in labelling and purification are required. They expected that non-insidious studies of protein production through ribosomal activity by means of PET can turn out to be a significant apparatus for therapy management and aim at classification for therapy and explained that <sup>44</sup>Sc-labeled puromycin-based DOTA-conjugates could be used for imaging of ribosomal operation and thus protein production in vivo.

Połosak *et al.* 2012,<sup>25</sup> carried out a study to estimate acrylic ligands necessary to be used for labelling proteins for instance monoclonal antibodies and their components with scandium radionuclides. Owing to the denaturation of proteins at temperature beyond 42°C, ligands, which capably build compounds at room temperature, are required for labelling. Radionuclides open chain ligands 1,2-bis(*o*-aminophenoxy)ethane-*N,N,N',N'*-tetraacetic acid (BAPTA), diethylenetriaminepentaacetic acid (DTPA), triethylenetetramine-*N,N,N',N'',N''',N''''*-hexaacetic acid (TTHA), *N,N'*-di(2-hydroxybenzyl)ethylenediamine-*N,N'*-

diacetic acid (HBED), ethylenebis(oxyethylenedinitrilo)-tetraacetic acid (EGTA), and deferoxamine was preferred in their study for complexation of scandium (**Figure 1.2**). They concluded that except HBED, the ligands build up tough complexes in ten minutes and the radiolabelling product differs between ninety-six and ninety-nine percent. The radiolabelling studies with no-carrier-added  $^{47}\text{Sc}$  posited that EGTA legends and 8-dentate DTPA produce the majority of steady complexes.<sup>25</sup>

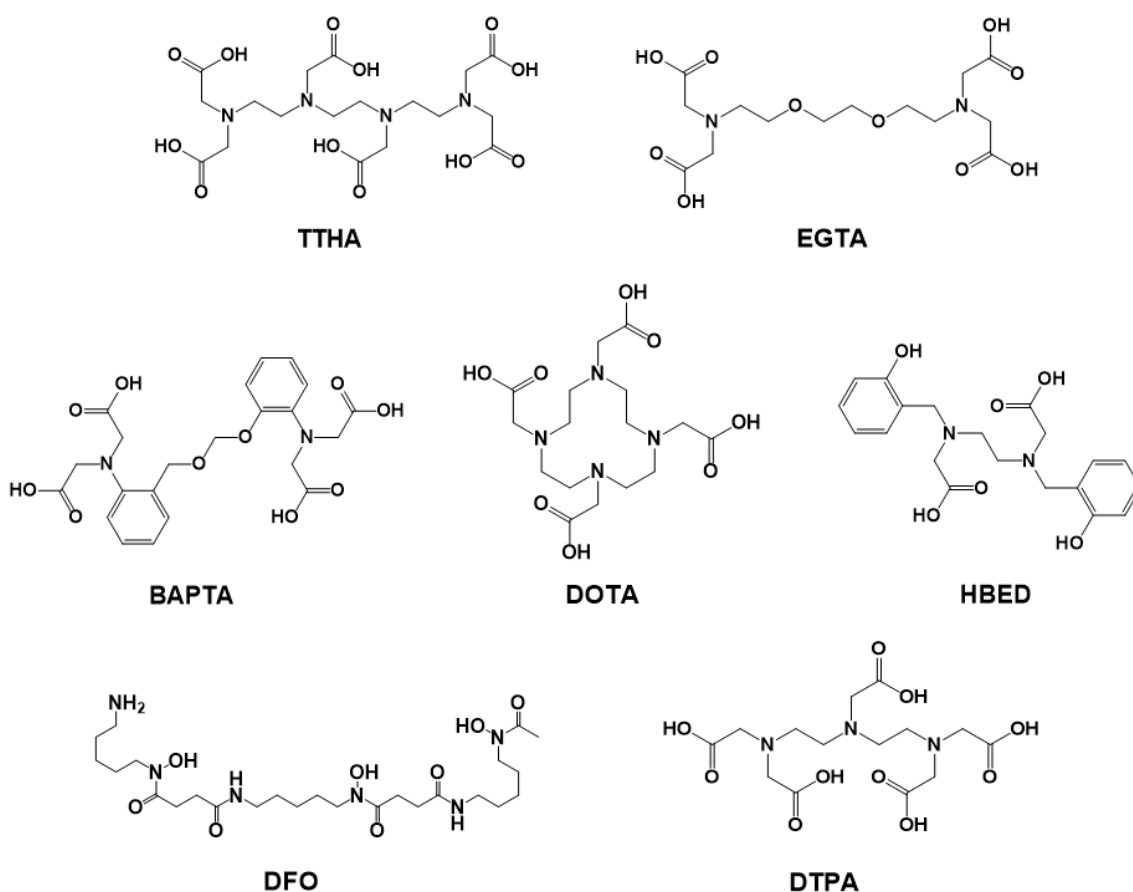


**Figure 1.2.** Structure of Połosak *et al.* ligands.

## 1.4. Calixarenes

The calixarenes are a group of organic macrocyclic host molecules, formed by the *ortho*-condensation of *para*-substituted phenols, by formaldehyde, generally in the existence of inorganic bases despite the fact that more rarely acid-catalysed cyclisation reactions are applied.<sup>44</sup>

### 1.4.1. History

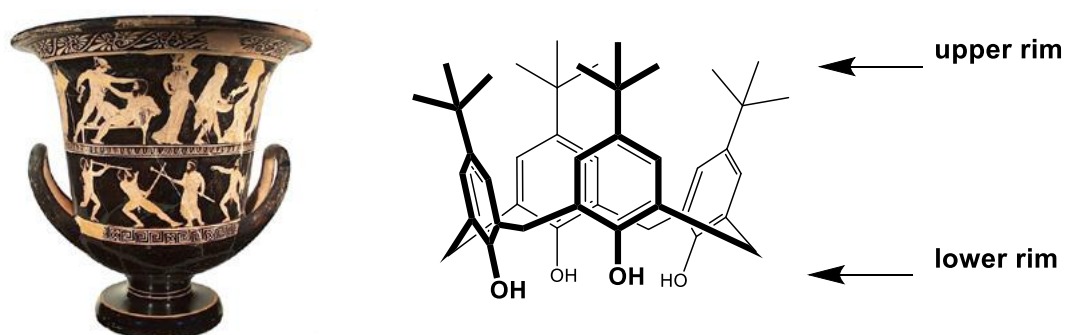
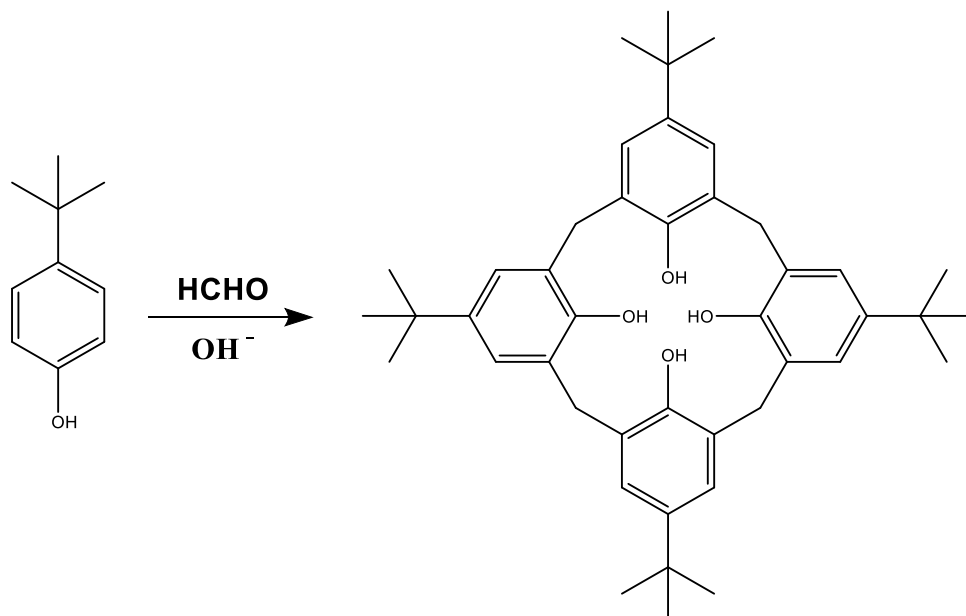


**Figure 1.3.** Greek Calyx krater vase on the left and Calixarene on the right

In 1872, Adolph von Bayer published the first results concerning the products obtained from the reaction of phenol with formaldehyde. In spite of numerous efforts, von Bayer was incapable of isolating or characterizing the products from this reaction, simply describing them as a substance that resembles cement.<sup>45</sup>

In 1894 consequently, Lederer and Manasse thrived in isolating from a similar reaction mixture, as *ortho*-hydroxymethylphenol, crystalline materials and *para*-hydroxymethyl phenol.<sup>46, 47</sup> The existence of both isomers crop up from the same activity in the reaction of *para* sites of phenol and the *ortho*. Ziegler and Zinke in 1944 abridged this problem of reactivity by blocking the *para*-site and with the use of *para-tert*-butylphenol. They recommended a cyclic structure for the formed product.<sup>48</sup> In 1957, the first report of a biomedical use of the calixarenes was in print by Cornforth, in which he illustrated the anti-tubercular properties of ethylene glycol derivatives of calixarenes.<sup>49</sup> At that time, the exact structural nature of the molecules lingered undetermined. Throughout the 1980s, a sequence of NMR reports by Gutsche helped resolve the macrocyclic nature of the calixarenes and the presence of cycles comprises four, six and eight phenolic units.<sup>50</sup> Gutsche was also the first to recommend the trivial name “calixarenes” for these molecules, through structural analogy with the figure of the ancient Greek Calyx krater vases (**Figure 1.3**). Given the complexity of the IUPAC terminology for the calixarenes, the name has lingered and currently, it is generally used. The basic nomenclature of the calixarenes uses [n] to designate the number of phenolic units in the macrocycle, therefore calix[4]arene has four.<sup>44</sup> The position and nature of substituents on the aromatic rings are given by sequential enumeration and the suitable term for the function is placed before the term calix[n]arene. Hydroxyl substitution once more follows the chronological numeration with a commonly substituent name located after calix[n]arene.<sup>44</sup>

### 1.4.2. Synthesis



The synthetic routes to the calixarenes are through multi-stage addition of phenolic units or by means of a single stage formation of a precursor and afterward cyclisation in order to obtain a preferred size of the macrocycle and subsequently a cyclisation.<sup>44</sup> Whereas the second method gives room for a reasonably easy way into calix[4]arenes having diverse roles at the *para*-positions, the synthesis is dreary and yields are usually low.<sup>44</sup> The one stage synthesis although it is restricted to producing symmetric molecules, (this is no longer a main setback in view of the advances in synthetic methodology for calix[*n*]arene amendment), is advantageous in proceeding to high yields for the macrocycles with eight, four or six phenolic units.<sup>44</sup> The *para*-substituents manipulate the macrocycle size and the yield. *Para-tert*-butylphenol generally serves as the main building block.<sup>51</sup>

For *para-tert*-butylphenol one stage cyclisation, the size obtained is selectively controlled by the combination of the reaction temperature

applied, the base catalyst and the solvent.<sup>44</sup> Generally, the purity of the acquired molecules is greater than 95%. Odd numbered macrocycles and higher numbered macrocycles are commonly acquired by means of HPLC purification of the mother liquors from the syntheses of the calix[4]arene or calix[8]arene are normally accessible in low yields < 5%.<sup>44</sup>

### 1.4.3. Properties

The dimensions of the calix[n]arenes and their approximate cavity sizes are normally smaller than common cyclodextrins.<sup>44</sup> The existence of methylene bridges that links the phenolic units in the calix[n]arenes results in conformational mobility in the molecules.<sup>44</sup> In 1985, Gutsche illustrated the existence of the four potential conformations of calix[4]arene.<sup>50</sup> The existence of bulky groups at the phenolic end, results in the blocking of conformational mobility.<sup>52</sup> The cone and alternate cone conformations can be created in a restricted manner with the use of appropriate cation templates in the substitution reactions.<sup>53</sup> When it comes to calix[6]arene,<sup>44</sup> eight conformations are achievable and a high degree of conformational mobility is there. There are two conformations that display an advanced stability, the alternate cone having three successive phenolic units that point in one direction and the other three in the contrary direction with reference to the plane of the molecule; the two groups of three consecutive units in the other case are crinkled into a pinched structure. Generally, this is present for the mono-substituted calix[6]arenes. When it comes to calix[8]arene,<sup>44</sup> 16 confirmations are achievable. The use of <sup>1</sup>H and <sup>13</sup>C NMR has permitted the study of the flexibility and conformational

nature of the calix[n]arenes. With reference to the calix[4]arenes, simple rules pertaining to the splitting patterns of the methylene protons and the chemical shift differences in the patterns allow relatively simple definition of the conformation of the macrocycles.<sup>54, 55</sup> The main predicament in using the calix[n]arenes in pharmaceutical or biomedical applications is completely lack of solubility of the parent molecules in aqueous systems and considerable synthetic attempt has been expended in acquiring either self-organising or water soluble systems for the same applications.<sup>44</sup>

#### **1.4.4. Chemical modification**

When contrasted with the cyclodextrins, the chemistry entailed in the modification of the calix[n]arenes is much simplified by the differences in the chemistry needed in substituting the phenolic hydroxyl groups or to carry out substitution at the *para*-position of the aromatic rings.<sup>44</sup> The chemistry of the modification of the calix[n]arenes has extensively been examined.<sup>52</sup>

##### **1.4.4.1. Water-soluble calixarenes**

The parent calixarenes confirm a successfully zero solubility in aqueous solution, and with no doubt this property is the one which held back the biopharmaceutical application of the calixarenes as compared to the crown ethers and cyclodextrins.<sup>44</sup> A variety of techniques has been built up since the 1980s to acquire water-soluble calixarenes. Ungaro *et al.*<sup>56</sup> discovered the first case in point of such compound in 1984, with

carboxylic acid groups coupled to the lower rim of calix[4]arene; the solubility in water was accomplished in the existence of Group 1 metal cations. The solubility ranged between  $5 \times 10^{-4}$  M and  $5 \times 10^{-3}$  in water dependent on the cation applied. In recent times, functions like phosphates, carboxylates, ammonium groups or sulfonates have been applied. Three probable locations for modification are present: at the phenolic functions, and by modification of the methylene bridges and by *para* to the phenolic groups.<sup>44</sup>

#### 1.4.4.1.1. Carboxylate functions

Amide functions and carboxylic acid have been applied at the *para*-positions and phenolic to stimulate solubility of water for the calixarenes **(Figure 1.4)**.<sup>57</sup> The high reactivity of the phenolic functions has generally made them the preferred location for such functionalization.<sup>58, 59</sup> The reaction is performed using simple treatment of an amide or a halo-alkyl ester in the existence of an appropriate base.<sup>60</sup> Selection of the base gives room for tetra-substitution or selective mono-, di-, tri- and the formation of cone or 1,3-alternate cone conformations in the derivatives is also directed by the nature of the base applied.<sup>61, 62</sup> Potassium or Sodium carbonate prefers the cone conformation of the calix[4]arene derivatives while the use of caesium carbonate results in the creation of the 1, 3-alternate isomers.<sup>44</sup>

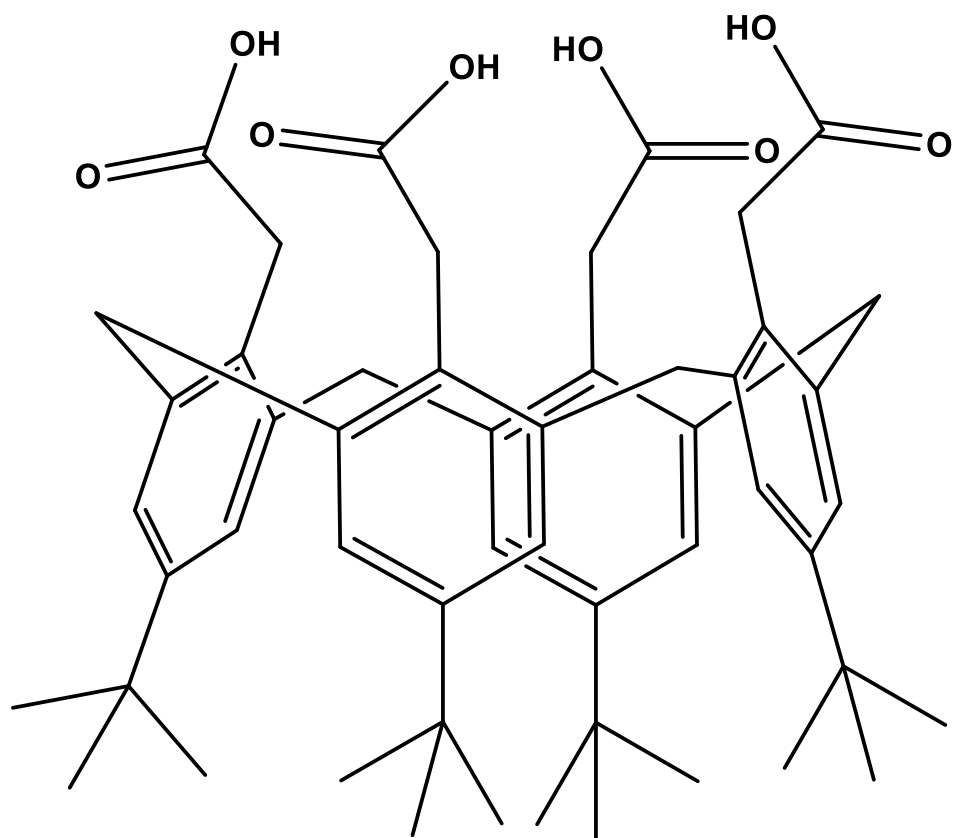


**Figure 1.4.** Structure of calix[4]arene with carboxylic acid function group at the phenolic end.

### 1.4.5. Biological activities

The capacity of the calixarene to complex a variety of molecules in the aqueous phase is fascinating for biological applications. Furthermore, they still possess the prospective to serve as direct bioactive molecules.<sup>44</sup>

#### 1.4.5.1. Toxicity of the calixarenes

A short account according to Gutsche in 1985 confirmed that the calixarenes had demonstrated no activity in the Ames test.<sup>57</sup> Perret *et al.* discovered that specific calix[4]arene phosphonate derivatives displayed no effects on the cell growth of human fibroblasts.<sup>63</sup> In the same abstract the authors discovered that giant vesicles rooted in amphiphilic phosphonato-calix[4]arene derivatives are capable of combining with the cell membranes of human fibroblasts but do not cause death of the cell. In recent times, Shahgaldian *et al.* have discovered that solid lipid nanoparticles founded on amphiphilic calix[4]arene derivatives display zero haemolytic effects at concentrations ranging up to 300 mg/l,<sup>64</sup> this is in contradiction of the behaviour of SLNs rooted in amphiphilic cyclodextrins which displays a momentous haemolytic impacts.<sup>65</sup> In the same way, Da Silva *et al.* have demonstrated that for a series of *para*-sulfonato-calix[8, 6 and 4]arenes and their haemolytic impacts, monosubstituted derivatives are experimental in the order *para*-sulfonato-calix[8]arenes > *para*-sulfonato-calix[6]arenes > *para*-sulfonato-calix[4]arenes, with 5% haemolysis taking place at concentrations of 20, 50 and 200 mM, respectively.<sup>66</sup> These results portray a preliminary demonstration of the exceedingly low levels of toxicity connected at the cellular level for the calix[n]arenes.

#### 1.4.5.2. Anti-tuberculosis calixarenes

One of the first tests on calixarene as an anti-tuberculosis agent took place in 1955 when Cornforth *et al.* performed tuberculostatic tests on *p*-*tert*-octylcalix[8]arene polyoxyethylene ether derivative (**Figure 1.5**).<sup>49</sup> The tests showed that calixarene has more anti-tuberculosis activity than Streptomycin, which was the gold standard TB treatment at the time.

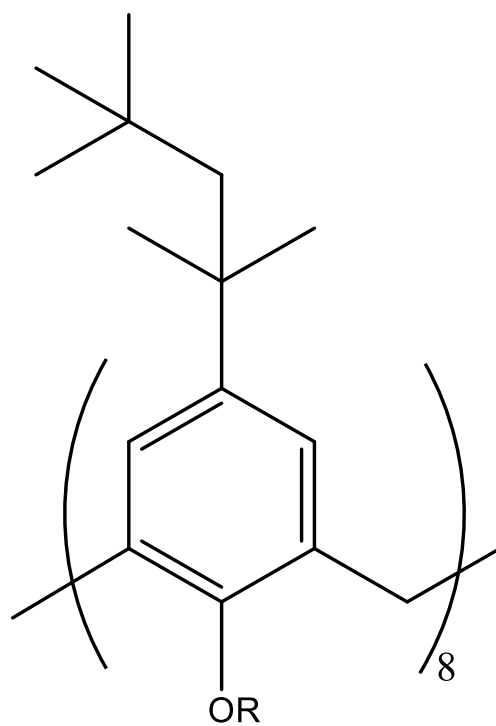


**Figure 1.5.** Polyoxyethylene ether *p*-*tert*-octylcalix[8]arene.

### 1.4.5.3. Anti-thrombotic calixarenes

Research has shown that water soluble sulfonated calixarenes has an anti-thrombotic activity.<sup>67</sup> Coleman *et al.* tested a number of sulfonated calixarene compounds, which he synthesised, for anti-thrombotic activity.<sup>68</sup> The results suggested that calixarene with carboxylic acid groups at the *endo*-rim have greater anticoagulant activity than non-functionalised sulfonatocalix[n]arene. The size of the calixarene was also found to have an effect on the anti-thrombotic activity. Hence, the larger the calixarene is, the higher the anti-thrombotic activity (**Figure 1.6**).

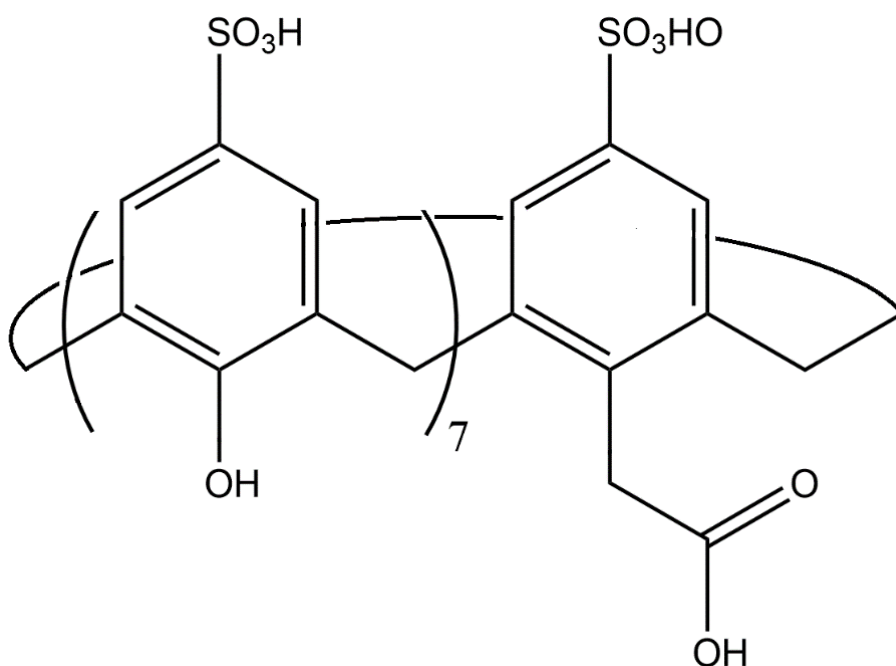


**Figure 1.6.** Structure of Coleman *et al.* compound that has the highest anticoagulant activity.

#### 1.4.5.4. Anti-viral calixarenes

In a study by Motornaya *et al.* investigating the anti-herpetic activity of calixarenes with aminoadamantane moieties at the upper rim, two compounds (**Figure 1.7**), were synthesised and tested to assess their anti-viral activities against the herpes simplex virus (HSV-2) cell line.<sup>69</sup> Aminoadamantanes have previously shown efficiency in both the treatment and prevention of viral infections.<sup>70</sup>

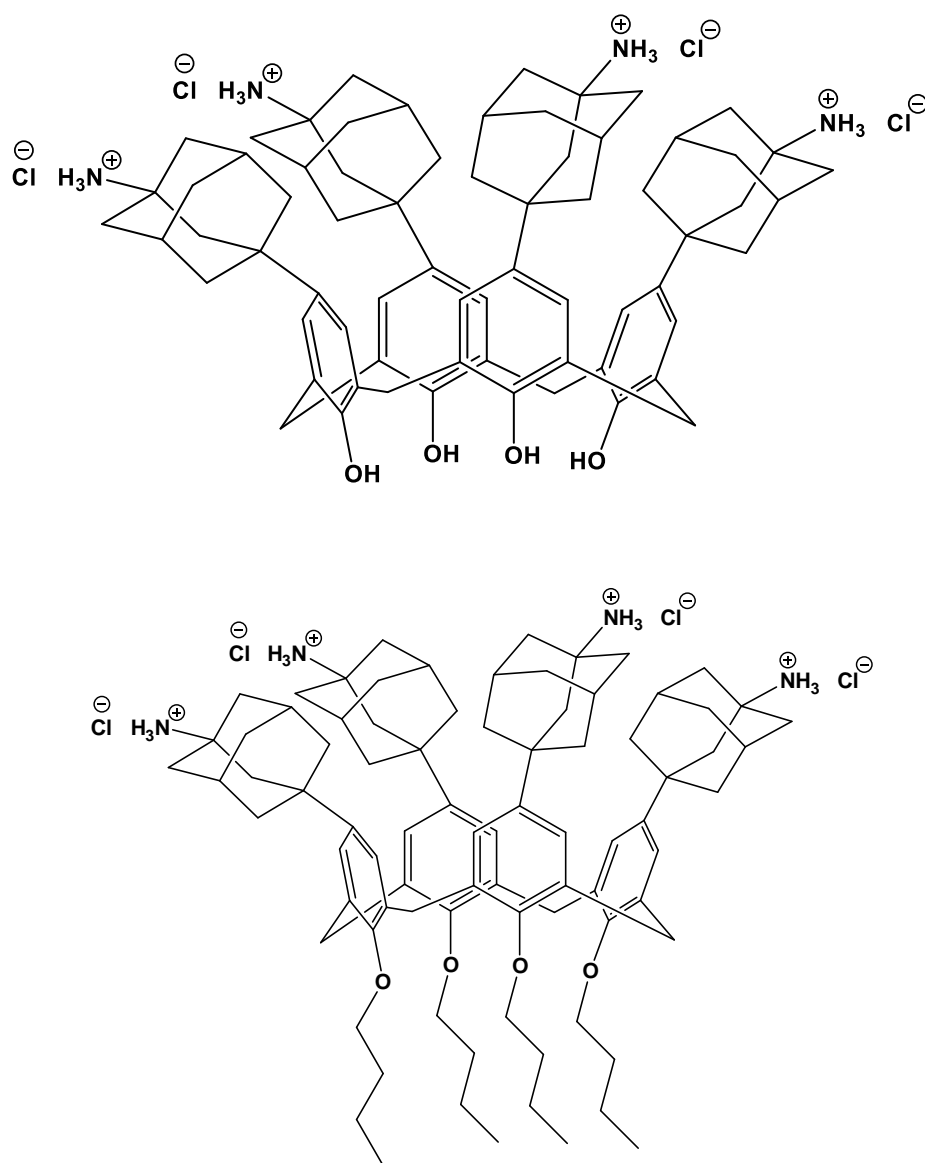


**Figure 1.7.** The structures of anti-herpetic agents by Motornaya *et al.*

According to their findings, the derivative with no modification at the lower-rim has a strong anti-viral activity. However, the chemotherapeutic safety index indicates that the compound is not safe enough for *in vivo* screening. For the compound where the lower-rim has been butylated, there was a weak or negative anti-viral activity. These results indicate that the phenyl hydroxyl groups play a role in the anti-viral activity of these two compounds, however that role has not been determined yet.

Another study by Hamilton *et al.* that supports the fact of calixarene having an anti-viral activity, selected calix[4]arene as a scaffold for anti-viral agent (**Figure 1.8**). The compound showed encouraging anti-viral activity against HIV virus.<sup>71</sup>

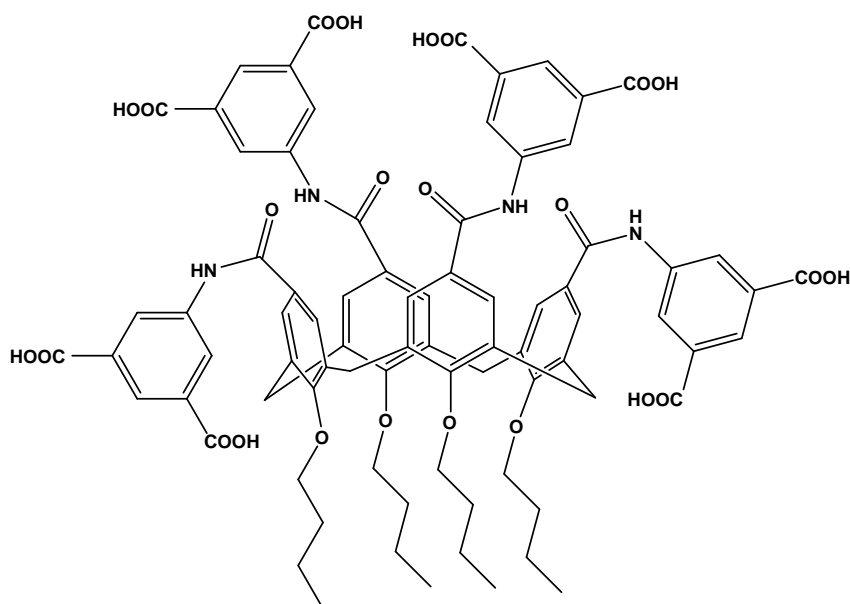


**Figure 1.8.** Hamilton's most promising anti-viral agent.

#### 1.4.5.5. Anti-microbial calixarenes

Casnati *et al.* in 1996 reported some of the first calixarene derivatives that was screened as antimicrobial agents.<sup>72</sup> One of the calixarene derivatives reported in Casnati study is shown in **(Figure 1.9)**. In a much larger study by Lamartine *et al.* 2002, the antimicrobial activity of 57 calixarene derivatives was measured by growth and inhibition rate comparisons against *Corynebacterium dematium*. Some of the compounds tested showed suitable antimicrobial activity.<sup>73</sup>

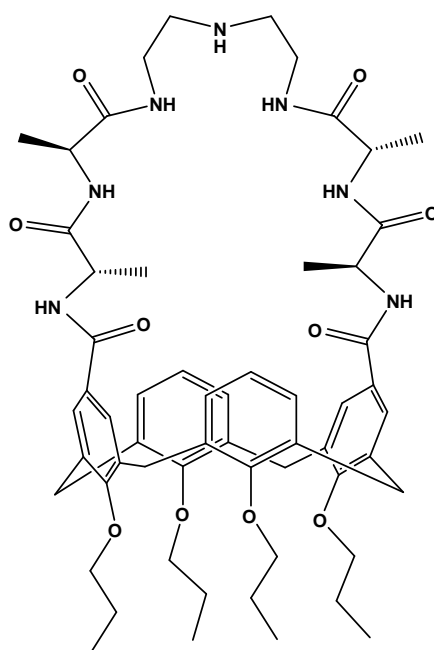


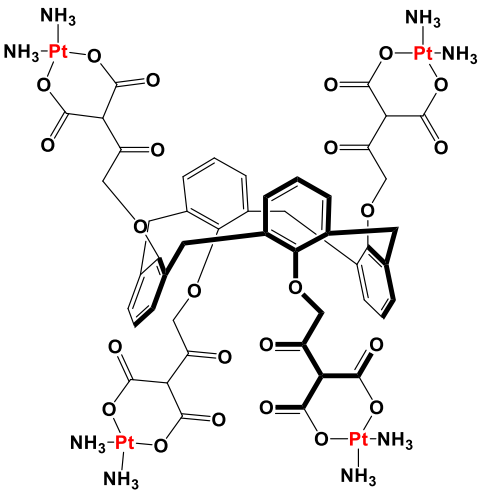
**Figure 1.9.** Antimicrobial calixarene derivatives reported by Casnati *et al.*

#### 1.4.5.6. Calixarenes as anti-cancer drugs

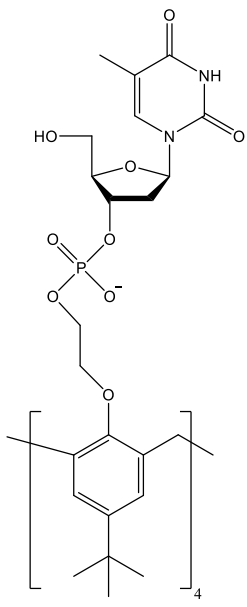
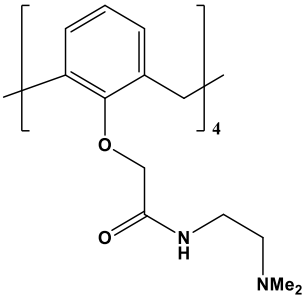
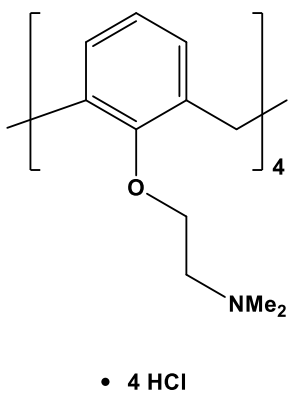
Calixarene-based compounds have been investigated by multiple research groups to study their anticancer activity. The therapeutic applications of calixarene and its derivatives has been an area of interest for some time. The geometric shape of calixarene enables it to carry the drug molecules by forming inclusion complexes and have the potential of controlled release, which might help in targeted chemotherapy. **(Table 1.1)** shows several examples of anticancer calixarenes:

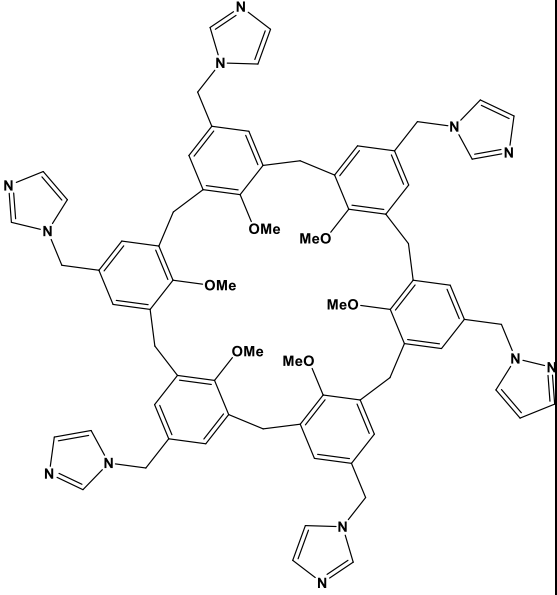
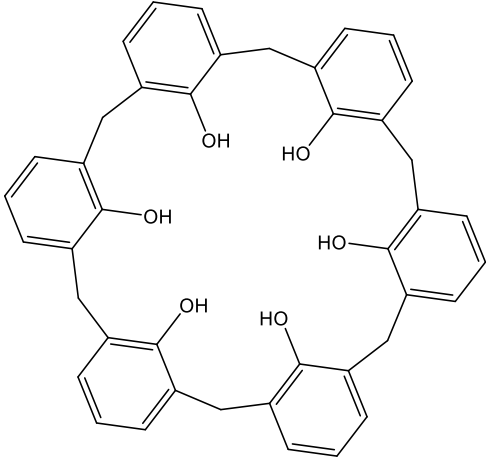
**Table 1.1**

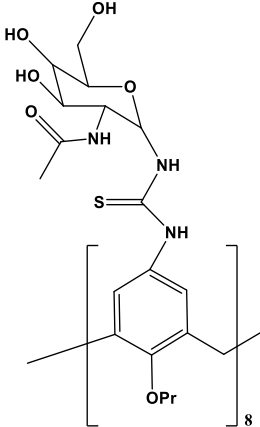
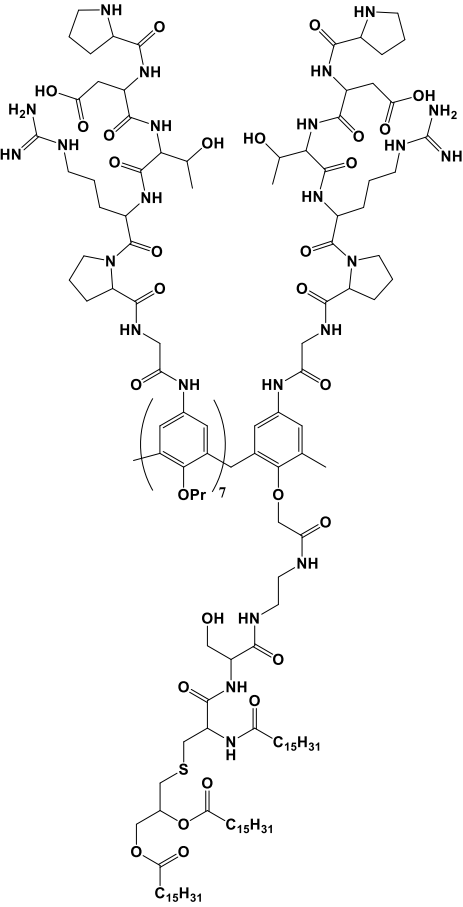
Examples of anti-tumour calixarenes

Type of calixarene	Structure	Mechanism of action	Reference
Calix[4]arene		Growth inhibitory	74

Type of calixarene	Structure	Mechanism of action	Reference
Calix[4]arene		Reduction in tumour growth	75
		Inhibit glutathione S-transferase and prevent multidrug resistance of cancer cells	76

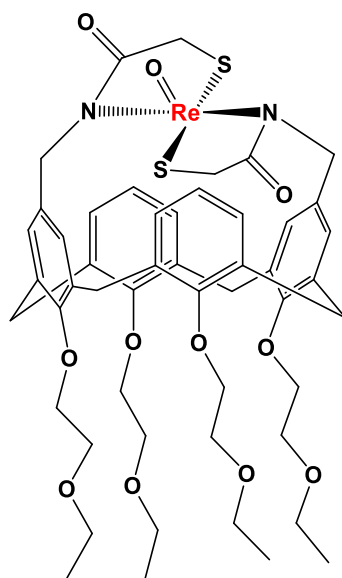
Type of calixarene	Structure	Mechanism of action	Reference
Calix[4]arene		Inhibition of DNA replication	77
		angiogenesis inhibitor	78
	 <p>• 4 HCl</p>	inhibiting tumour growth	79

Type of calixarene	Structure	Mechanism of action	Reference
Calix[6]arene		stabilize the p53 gene	80
		inducing cell death in human pancreatic cancer cells	81

Type of calixarene	Structure	Mechanism of action	Reference
Calix[8]arene		Prevent tumour migration and proliferation	82
		Stimulate B lymphocytes for antibody production	83

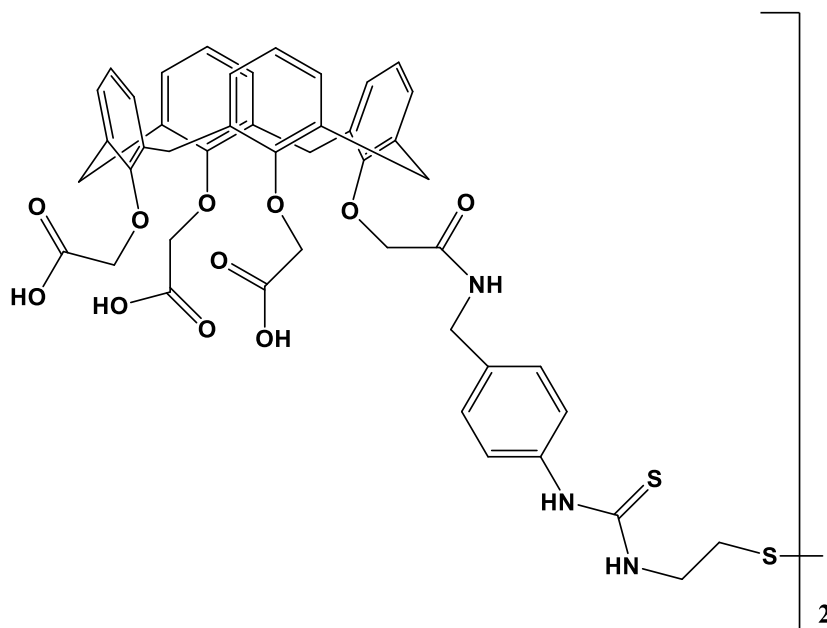
#### 1.4.5.7. Calixarene in radiotherapy

Ionizing radiation has been applied in the treatment of cancer for many years. In order to minimize the radiation damage to healthy cells, radioactive metal ions have to be complexed by strong chelators, which have antibodies or particular peptides that deliver the agent to cancer cells and therefore minimizing the damage of healthy cells. For this system to work, it is necessary to have bifunctional ligands that can form strong and stable connection to the targeting vector and the radionuclides. The most popular transition metals used for radiotherapy are  $^{99m}\text{Tc}$ ,  $^{186}\text{Re}$  and  $^{188}\text{Re}$ . Complex (**Figure 1.10**) was prepared to be used as a radiopharmaceutical, and it showed stability in PBS.<sup>84</sup>



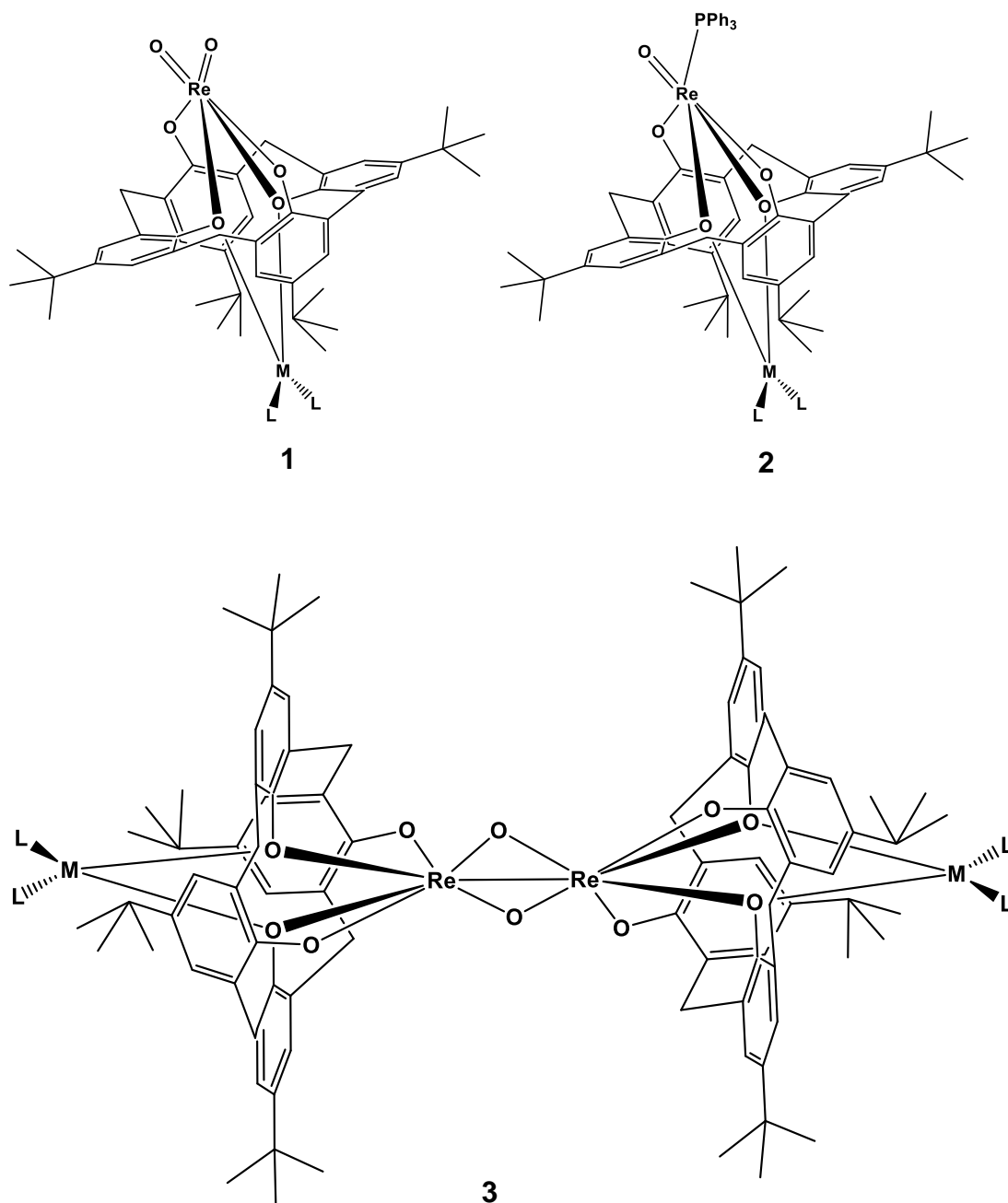
**Figure 1.10.** Re-calixarene radiopharmaceutical precursor.

An important isotope for radiotherapy is the  $^{225}\text{Ac}^{3+}$ , which has a 10 days half-life. The calixarene derivative shown in **(Figure 1.11)** was synthesised and their  $\text{Ac}^{3+}$  coordination was studied. Immunoreactivity and immunogenicity of this complex was reported.<sup>85</sup>



**Figure 1.11.** Structure of calixarene derivative for  $\text{Ac}^{3+}$  labelling.

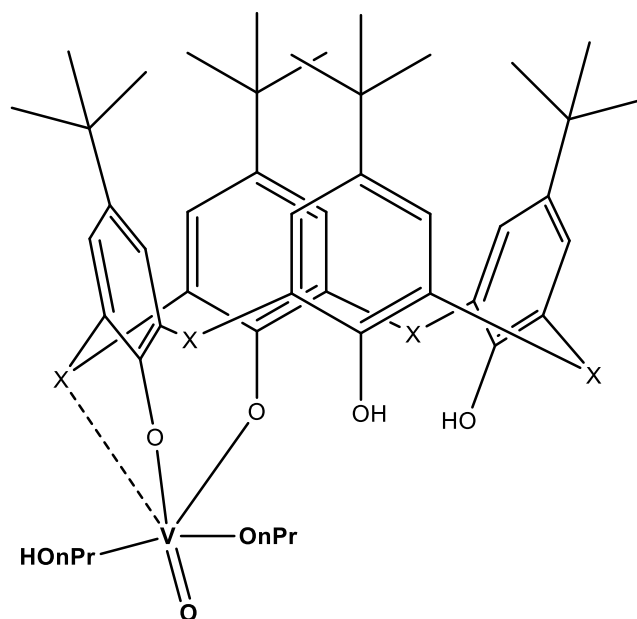
Redshaw *et al.* examined the chelation ability of calixarenes to rhenium and synthesised multiple rhenium calixarene complexes as precursors to medical imaging agents and cancer therapeutics.<sup>86</sup> Some of these complexes are shown in **(Figure 1.12)**.



**Figure 1.12.** Examples of rhenium calixarene complexes reported by Redshaw *et al.* M = Na/K, L = MeCN.

Complex **3** is the first rhenium-rhenium bond supported by calixarene ligands. However, due to the synthesis complexity and air sensitivity of these complexes, they cannot be used in biomedical applications.

In other research, Redshaw *et al.* reported structures of multiple vanadyl calixarene complexes and screened them against different cell lines.<sup>87</sup> The toxicity varied in the different cell lines from non-toxic to IC50 values of 0.1  $\mu\text{M}$ . This gave evidence of selective cell type toxicity. Cellular uptake of these complexes was slow with no noticeable uptake after 15 min. after 3-4 hours however, saturation took place. **(Figure 1.13)** is an example of Redshaw's vanadyl calixarene complexes.

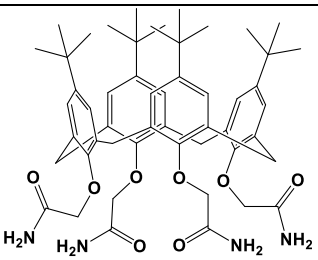
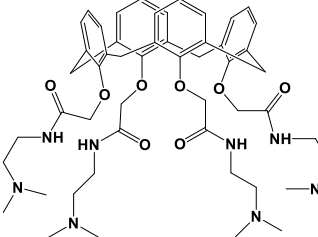
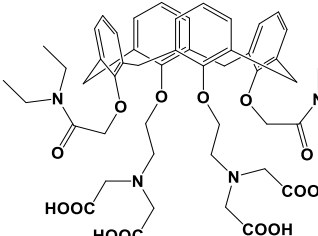
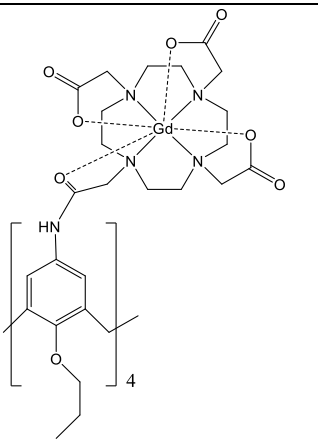
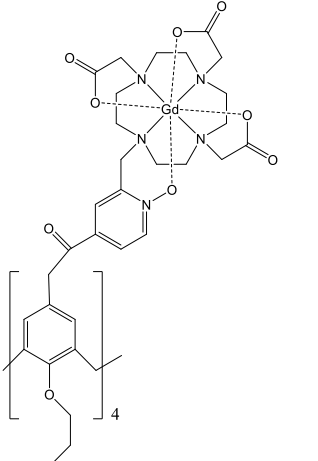


**Figure 1.13.** The structure of Redshaw's vanadyl calixarene complex.  
X = SO<sub>2</sub> (i.e. sulfonyl).

#### 1.4.5.8. Calixarenes as MRI contrast agents

Gadolinium complexes are the most dominant contrast agents for MRI as the Gd(III) ion is very efficient at accelerating the relaxation time of hydrogen ions in water.<sup>88</sup> Gd(III) in its free ion state is very toxic *in vivo*, therefore, it is crucial to use it in a very stable complexes that ensure the Gd(III) ion will not detach from the ligand.

In **(Table 1.2)** a list of calixarenes that has been synthesized and investigated as chelators for Gd(III) ions for the purpose of making MRI contrast agents candidates.

Structure	Relaxivity value	stability constant	Reference
	3.4 mM <sup>-1</sup> s <sup>-1</sup> at 400 MHz in a mixture of water and DMSO	1x10 <sup>3</sup> M <sup>-1</sup>	89
	Unknown	2x10 <sup>5</sup> M <sup>-1</sup>	90
	9.6 mM <sup>-1</sup> s <sup>-1</sup> at 20 MHz and 25°C	1x10 <sup>13</sup> M <sup>-1</sup>	91
	18.3 mM <sup>-1</sup> s <sup>-1</sup> at 20 MHz and 37°C	1.2x10 <sup>3</sup> M <sup>-1</sup>	92
	125 s <sup>-1</sup> mM <sup>-1</sup> at 20 MHz and 25 °C	Unknown	93

**Table 1.2.** Calixarenes as a MRI contrast agents

## 1.5. Known Scandium calixarenes

In the past decade, extraction selectivity and calixarene complexability towards rare earths has been demonstrated to be extremely interrelated amid the fit between the cation, the conformational functional groups and the cavity size.<sup>94</sup> Sc-calixarene complexes however, have rarely been synthesized. To the best of my knowledge the following complexes are the only Sc-calixarene complexes reported to date.

The first oxa-calix[3]arene Sc complex X-ray structure was discovered in 1995 (**Figure 1.14**).<sup>95</sup> It demonstrated that the Sc complex comprises a structure having coordination number 6. In order to expand the calixarene complexing reactions to Sc, Yawen Zhanga *et al.*, 1998, came up with three Sc and *p-tert*-butylcalix[*n*]arenes complexes (*n* = 4,6,8).<sup>96</sup> Their complexes behave as 1:1 and 1:2 electrolytes for calix[4,6]arene and calix[8]arene respectively.

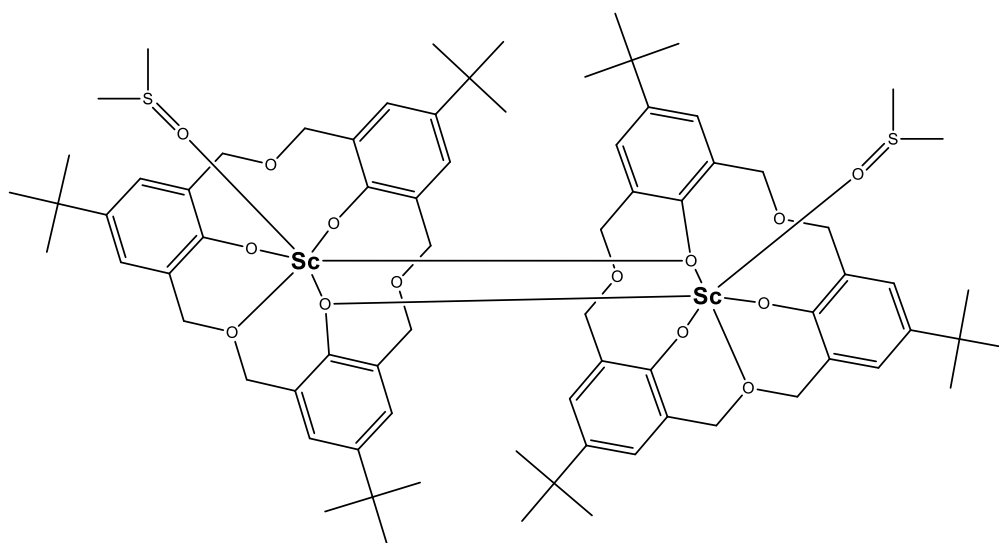


**Figure 1.14.** The first oxa-calix[3]arene Sc complex X-ray structure.

Webb, *et al.* 2001, reacted sodium *p*-sulfonatocalix[4]arene and scandium (III) tristriflate, which gave the complex (**Figure 1.15**).<sup>97</sup> The reaction was also done in the presence of [18]crown-6 and gave the complex (**Figure 1.16**).

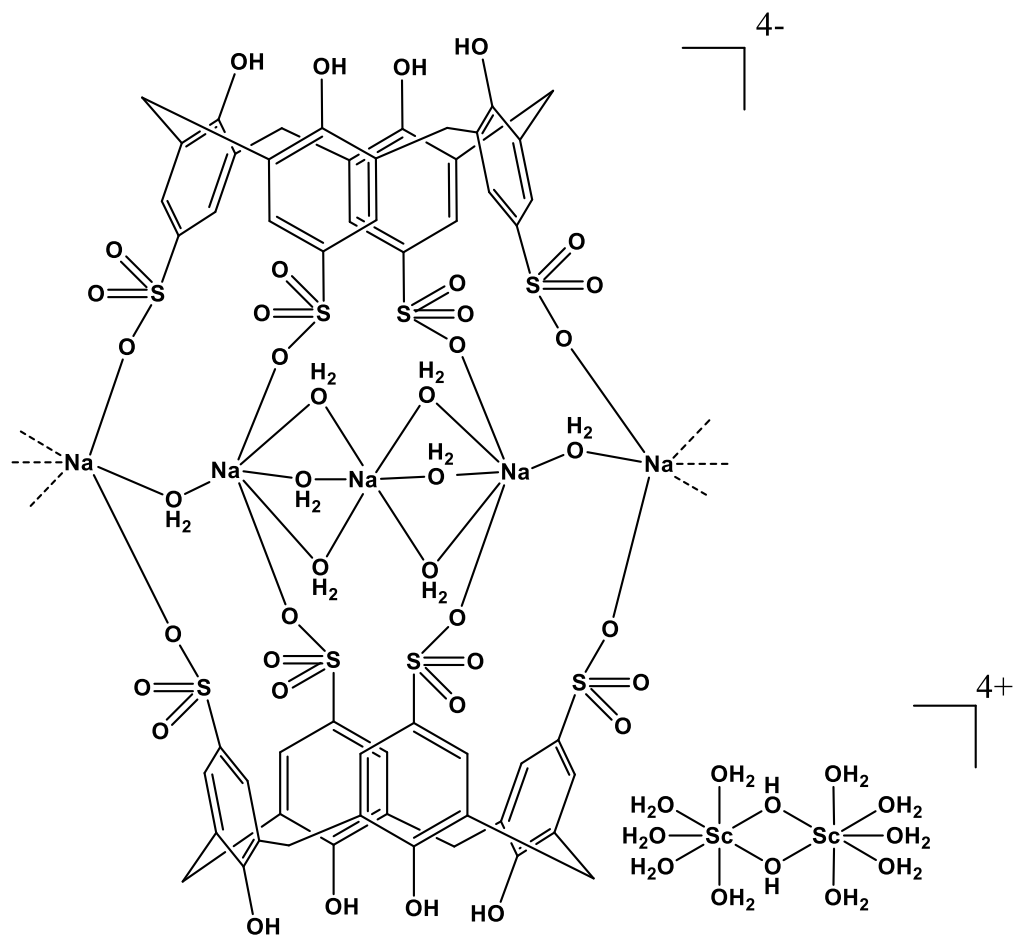


**Figure 1.15.** Structure of Webb, *et al.* scandium calix[4]arene complex in the absence of [18]crown-6.

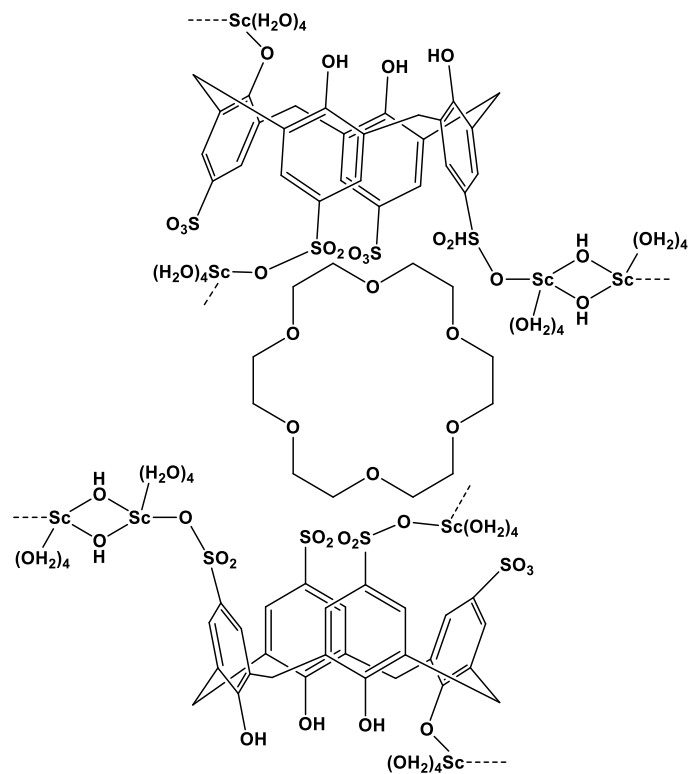


**Figure 1.16.** Structure of Webb, *et al.* scandium calix[4]arene complex in the presence of [18]crown-6.

Gou, *et al.* 2007, synthesized scandium *p-tert*-butylcalix[6]arene complex from scandium isopropoxide (**Figure 1.17**).<sup>98</sup>

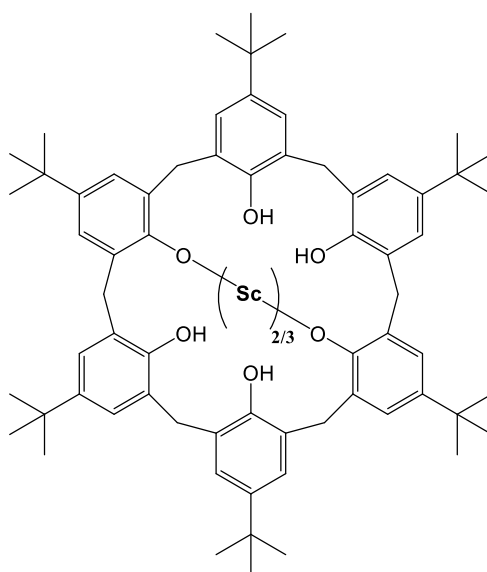


**Figure 1.17.** Structure of Gou, *et al.* scandium calix[6]arene complex.

Estler, *et al.* 2002. Synthesized the complex in **(Figure 1.18)**. 25,27-O-Benzylated-calix[4]arenes H<sub>2</sub>L reacted with Sc-[N(SiHMe<sub>2</sub>)<sub>2</sub>]<sub>3</sub>(THF) to yield monomeric calix[4]arene complex with a N(SiHMe<sub>2</sub>)<sub>2</sub> ligand bonded to the scandium atom.<sup>99</sup>

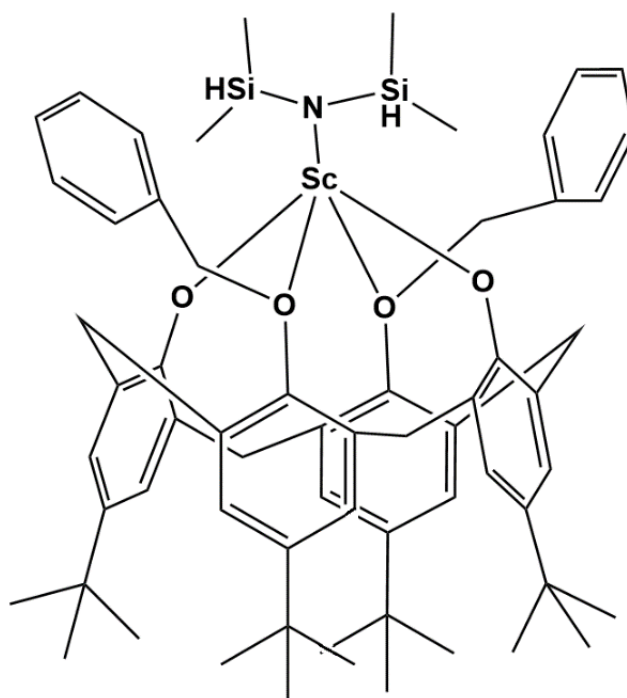


**Figure 1.18.** Structure of scandium calix[4]arene complex reported by Estler *et al.*

## **Chapter 2**

### **Results and Discussion**

## 2.1. Aims

In this chapter, I detail the five complexes synthesized in this project. The first section of this chapter details the synthesis and crystal structures of two scandium complexes based on *p*-*tert*-butylcalix[4]arene. The second section details the synthesis and crystal structure of one scandium complex and lithium chloride complex based on *p*-*tert*-butylcalix[6]arene. The third section details the synthesis and crystal structure of a scandium complex based on *p*-*tert*-butylcalix[8]arene. (See **figure 2.1** for the calixarenes used)

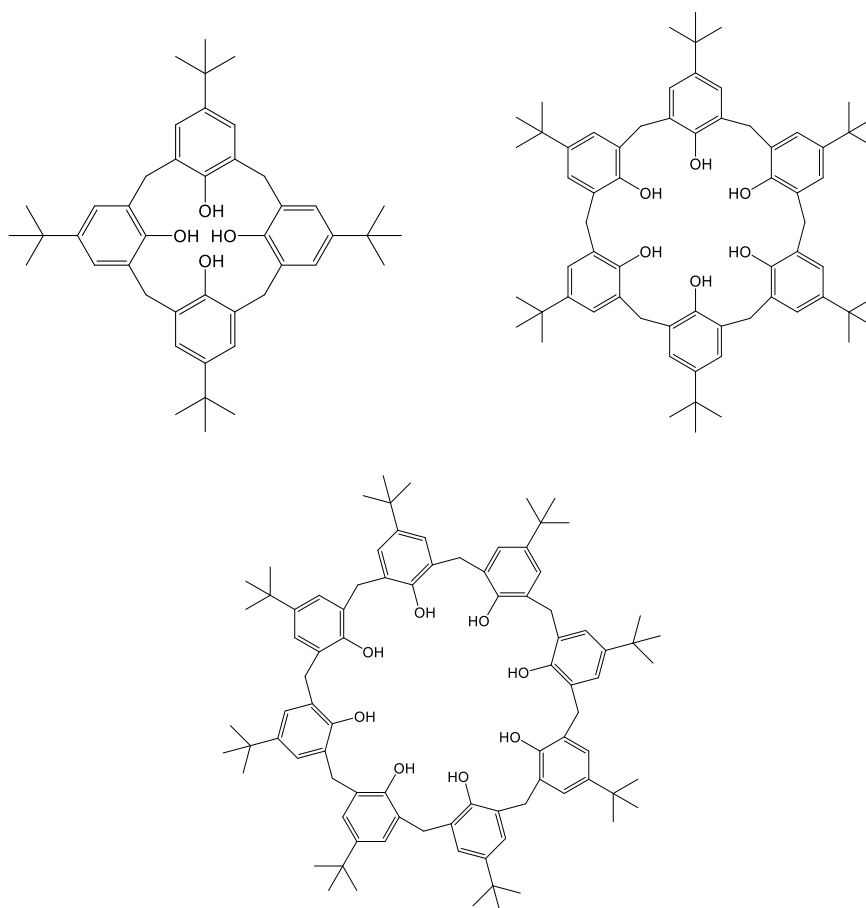


**Figure 2.1.** The chemical structures of the three ligands used in this work.

## 2.2. *p*-*tert*-butylcalix[4]arene chemistry

2.2.1. Interaction of 4-*tert*-butylcalix[4]arene with two equivalents of scandium(III) isopropoxide in toluene afforded the complex  $[(\text{calix-4})_6\text{Sc}_9(\text{OH})_8(\text{MeCN})_4]\cdot 11\text{MeCN}$  (**1**). Recrystallization from a saturated acetonitrile solution on prolonged standing at room temperature led to the formation of colourless crystals suitable for a single crystal X-ray diffraction study. Yield 7.9%. The molecular structure of (**1**) is shown in (Figures 2.2-2.4). X-ray data is attached in the appendix.

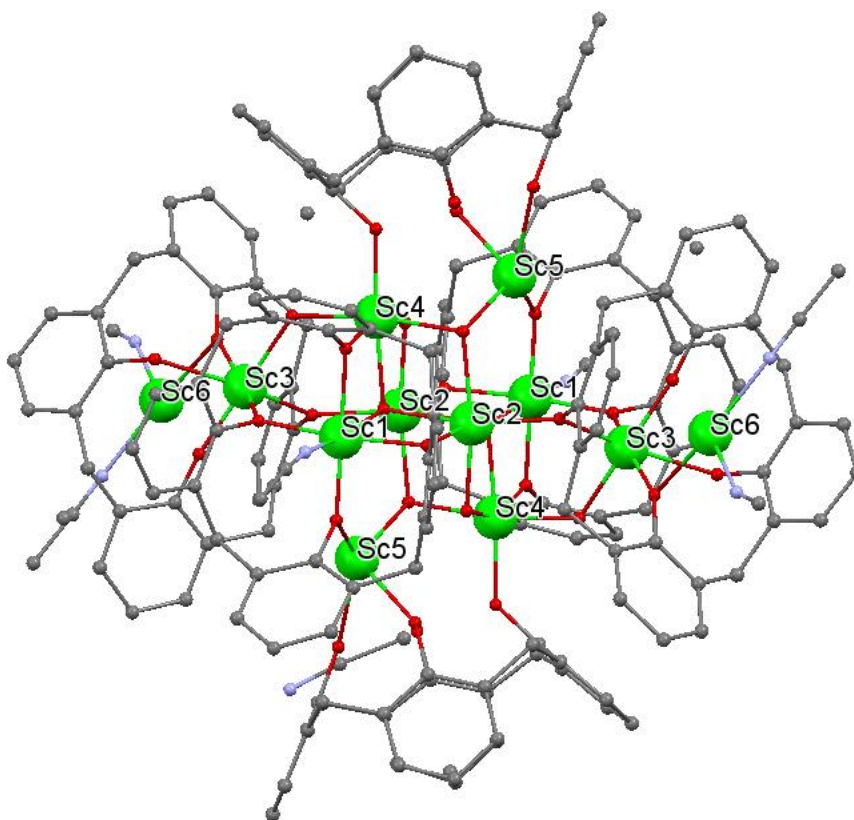


**Figure 2.2.** First view of complex (**1**) molecular structure. The hydrogen atoms and the *t*-butyl groups of calixarenes are removed for clarification. Selected bond lengths (Å) and angles (°): O1-Sc1 2.110(3), O2-Sc1 1.957(3), O3-Sc1 2.142(3), O4-Sc1 2.110(3), Sc1-Sc2 3.1939(9), Sc1-Sc5 3.654(4); O2-Sc1-O1 94.02(11), O2-Sc1-O4 174.03(10), O1-Sc1-O4 87.98(10), O2-Sc1-O3 90.69(11), O1-Sc1-O3 174.84(10), O4-Sc1-O3 87.54(10), O2-Sc1-Sc2 96.23(8), O1-Sc1-Sc2 136.41(7), O4-Sc1-Sc2 86.14(7), O3-Sc1-Sc2 40.61(6), O2-Sc1-Sc5 32.53(9).

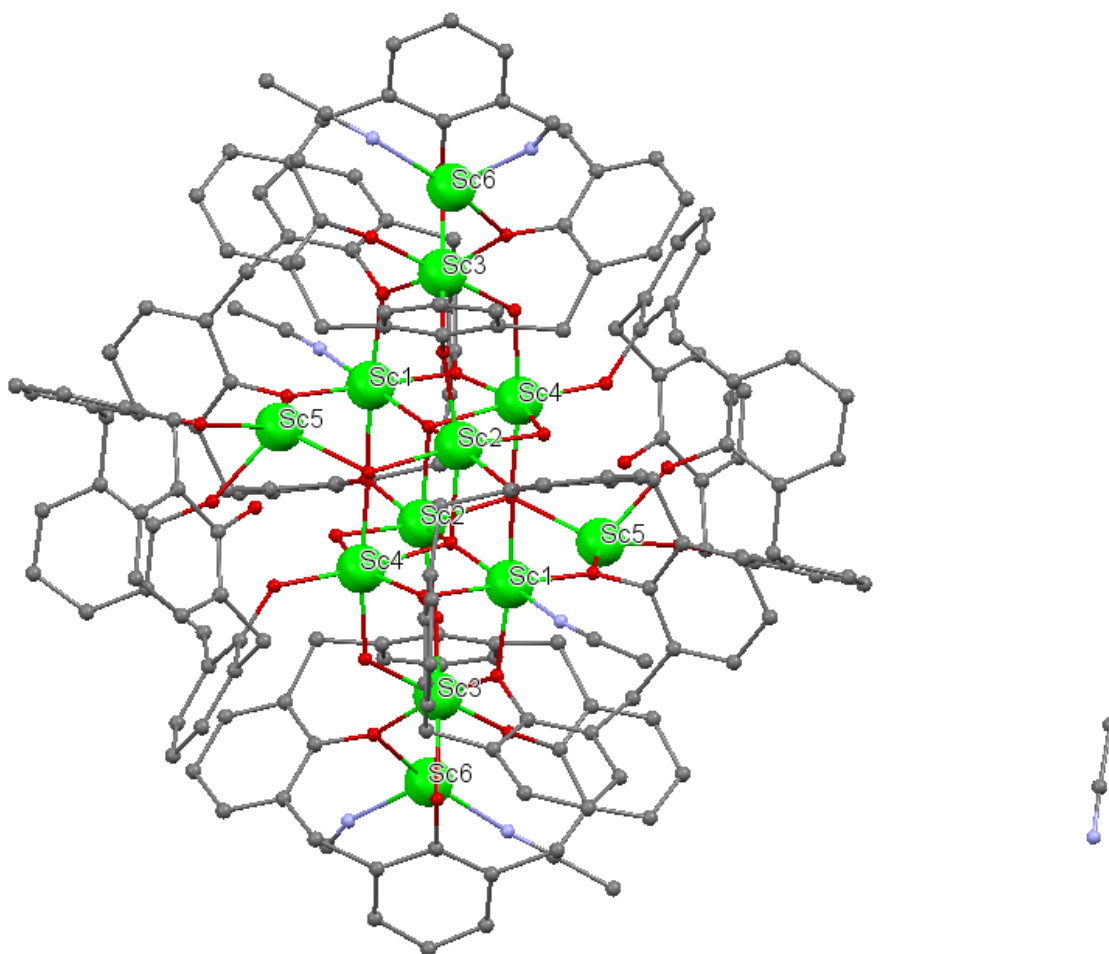


**Figure 2.3.** Alternative view of complex **(1)**. The hydrogen atoms and the *t*-butyl groups of calixarenes are removed for clarification.

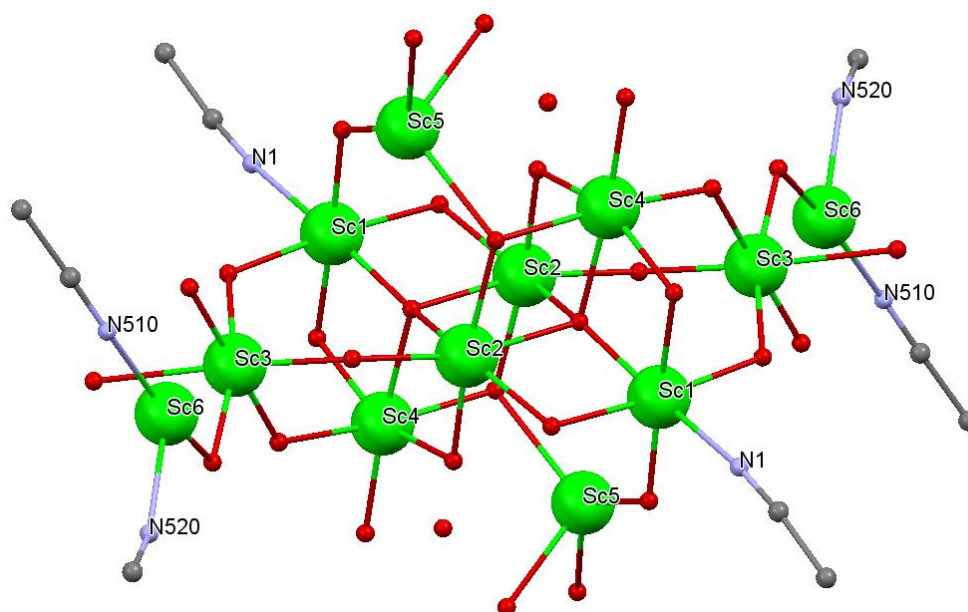


**Figure 2.4.** A view of the core of complex **(1)**. calix[4]arenes are removed for clarification.

The compound crystallises within a huge unit cell (volume  $\sim 28610 \text{ \AA}^3$ ) with a massive asymmetric unit and  $Z=8$  in space group  $C2/c$ .

The structural formula is approximately (calix-4- $\text{H}_2$ ) $_6\text{Sc}_9(\text{OH})_8(\text{MeCN})_4 \cdot 11\text{MeCN}$ , however, it is not clear from the diffraction data exactly how many of the hydroxide anions should be formulated as oxide.

The cluster is centrosymmetric and contains a central core of four  $\text{ScO}_6$  distorted octahedra and two distorted  $\text{ScO}_5\text{N}$  octahedra that share edges. These are capped by further  $\text{ScO}_6$  distorted octahedra that share corners with the other six. There are further Sc ions surrounding this block that are partially occupied and have a coordination number four. The refinement is not better if these sites are occupied by lithium. The cluster is surrounded by six calix[4]arene molecules four of which are completely deprotonated and the oxygen atoms coordinate to the Sc ions; the other two have a single proton only and coordinate through the oxygen atoms. To emphasise the structure one might formulate this as [(calix-4) $_6(\text{ScOH})_8\text{Sc}_1(\text{MeCN})_4 \cdot 11\text{MeCN}$  where the cluster is enclosed in square brackets. The coordination about the Sc is completed by MeCN. There is further ordered MeCN that is not bound to Sc and other disordered solvent. The structure refinement was completed using the SQUEEZE routine within PLATON to model disordered solvent. This gives the 11MeCN per formula unit. Seven of these are ordered and four of these disordered.

2.2.2. Interaction of 4-*tert*-butylcalix[4]arene with scandium(III) isopropoxide in toluene afforded the complex  $[\text{Sc}_4\text{O}(\text{calix-4})_4] \cdot 12\text{C}_6\text{H}_5\text{CH}_3$  (**2**). Recrystallization from a toluene and acetonitrile on prolonged standing at room temperature led to the formation of colourless crystals suitable for a single crystal X-ray diffraction study. Yield 20.2%. The molecular structure of (**2**) is shown in (Figures 2.5-2.8). X-ray data is attached in the appendix.

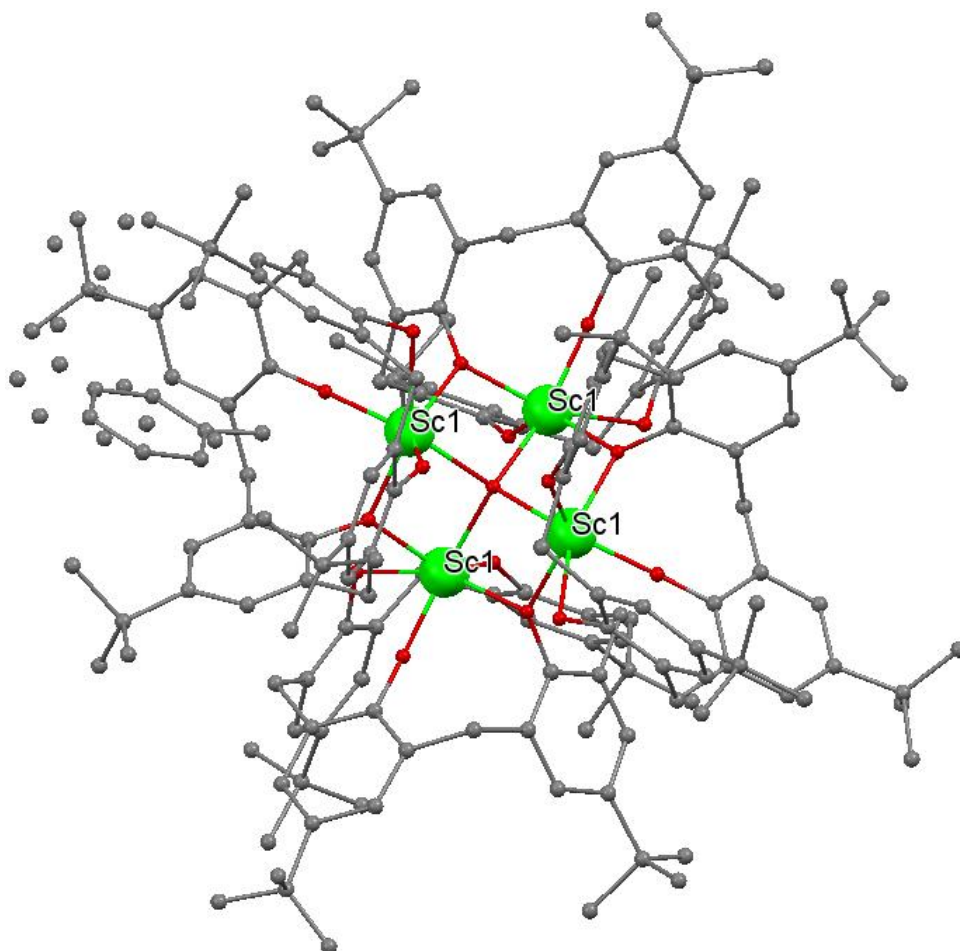


**Figure 2.5.** First view of complex (**2**) molecular structure. The hydrogen atoms are removed for clarification. Selected bond lengths (Å) and angles (°): O1-Sc1 2.094(2), O2-Sc1 1.932(2), O3-Sc1 2.432(2), O4-Sc1 2.021(2), O5-Sc1 2.1746(5); O2-Sc1-O4 115.29(10), O2-Sc1-O1 86.65(9), O4-Sc1-O1 92.02(9), O2-Sc1-O5 148.45(7), O4-Sc1-O5 91.89(8), O1-Sc1-O5 76.16(6), O2-Sc1-O3 77.12(8), O4-Sc1-O3 77.37(8), O1-Sc1-O3 154.18(8), O5-Sc1-O3 126.99(6).

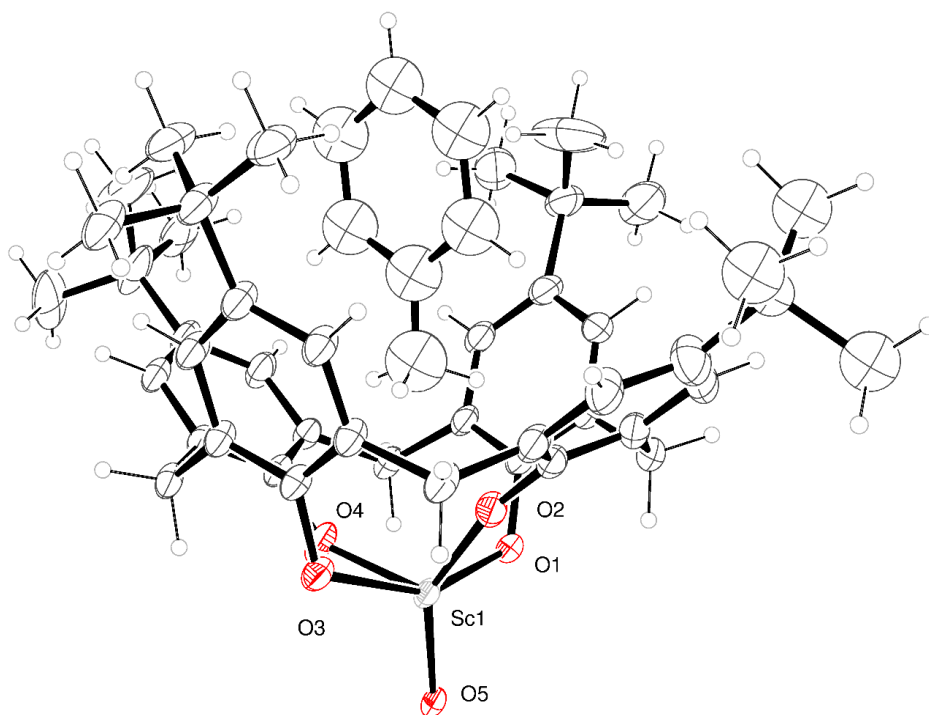


**Figure 2.6.** Molecular structure of complex **(2)**. Asymmetric unit with atoms drawn as 30% probability ellipsoids.

There is a single Sc ion in the asymmetric unit. It is coordinated by the four oxygen atoms of the calixarene and another oxide (O5). Four of these units are arranged in a cluster that is centred on O5. The atom O1 bridges between symmetry-related scandium ions. O5 is surrounded by four scandium ions in a flattened tetrahedral arrangement (Sc1–O5–Sc1\_i 101.033(11)° and Sc1–O5–Sc1\_iii 128.11(3)°)

Within the bowl of each calix-4 is located a disordered toluene molecule. The clusters have composition  $\text{Sc}_4\text{O}(\text{calix-4})_4$  and these are packed in a rather open arrangement; channels run parallel to the [100] and [001] directions. These are filled with disordered toluene which was modelled using the SQUEEZE routine to give a composition of  $\text{Sc}_4\text{O}(\text{calix-4})_4 \cdot 12\text{C}_6\text{H}_5\text{CH}_3$ .

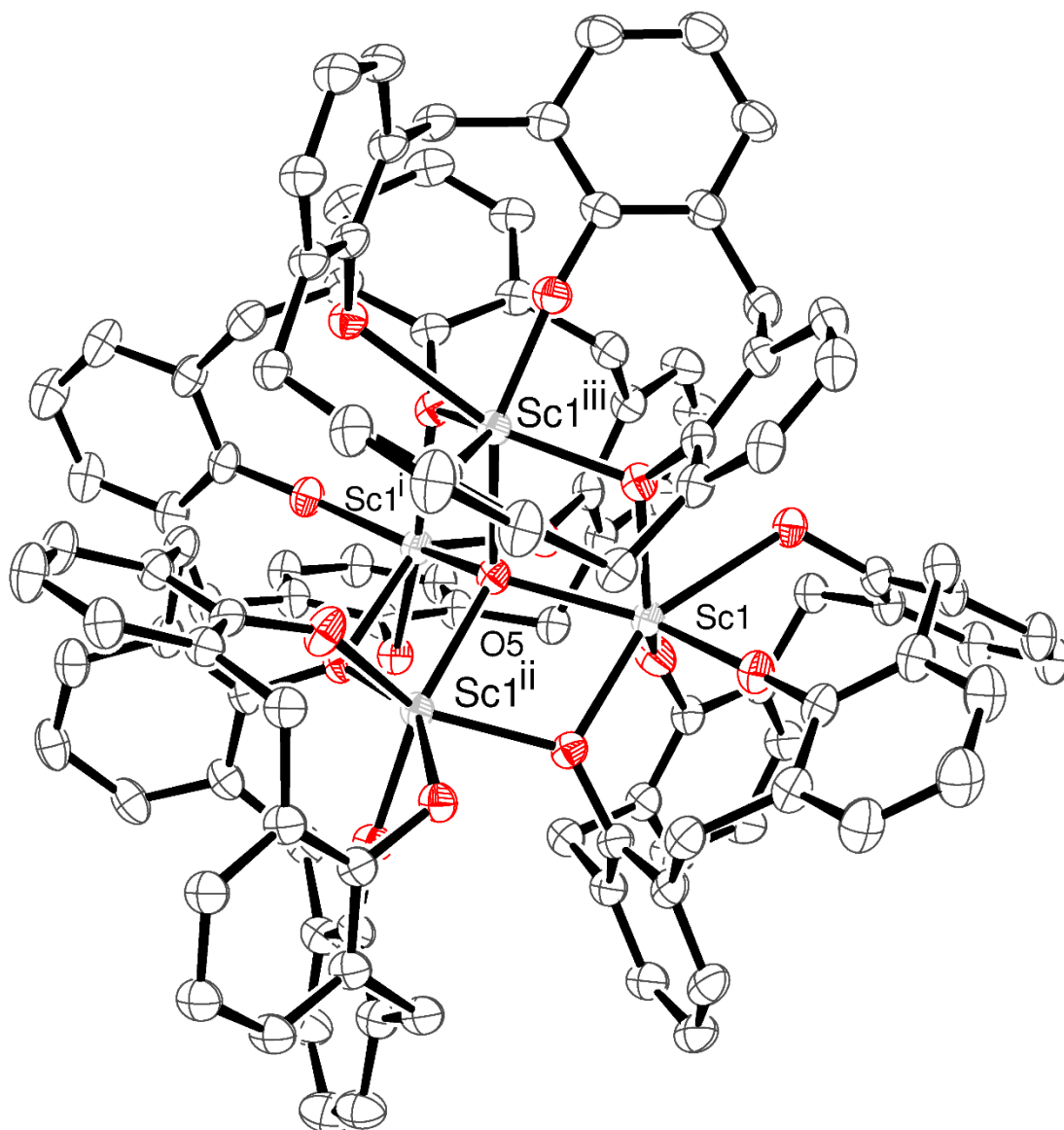


**Figure 2.7.** Alternative view of complex **(2)**. A single  $\text{Sc}_4\text{O}(\text{calix-4})_4$  cluster. For clarity, hydrogen atoms and *t*-butyl groups are not shown. Operators used to generate symmetry-equivalent atoms:  $i = 1.5 - y, x, 0.5 - z$ ;  $ii = y, 1.5 - x, 0.5 - z$ ;  $iii = 1.5 - x, 1.5 - y, z$ .

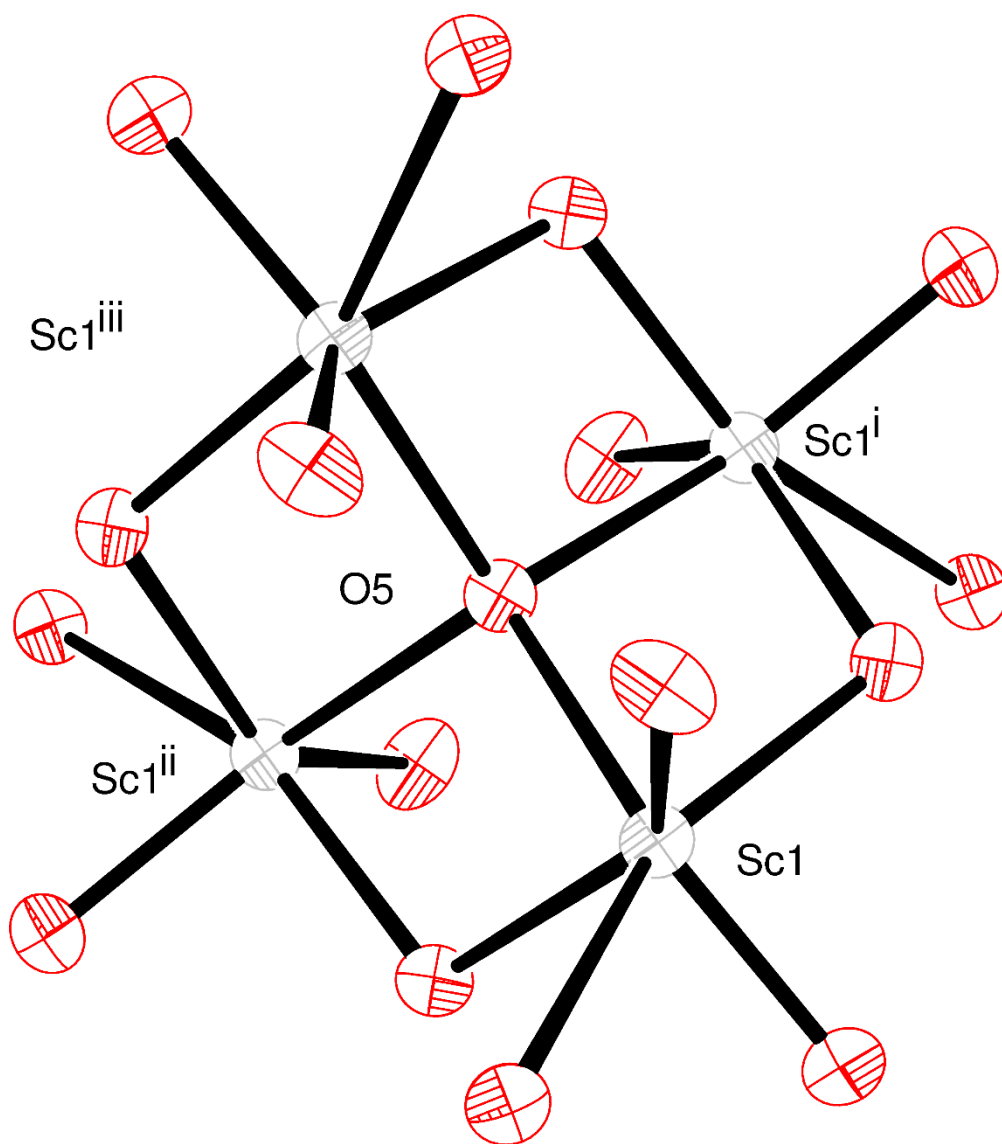


**Figure 2.8.** Core of complex **(2)**. For clarity, only the Sc and O atoms are shown. Operators used to generate symmetry-equivalent atoms: i =  $1.5-y, x, 0.5-z$ ; ii =  $y, 1.5-x, 0.5-z$ ; iii =  $1.5-x, 1.5-y, z$ .

## 2.3. *p*-*tert*-butylcalix[6]arene chemistry

### 2.3.1. Interaction of 4-*tert*-butylcalix[6]arene with scandium(III)

isopropoxide in toluene refluxing for 24 hours afforded the complex  $[\text{Sc}_4\text{O}(\text{calix-6})_2]\text{C}_8\text{H}_{12}\text{N}_4\text{Na}0.5(\text{C}_6\text{H}_9\text{N}_3\text{Na})\cdot 6\text{MeCN}$  (**3**). Recrystallization from a saturated acetonitrile solution in 0 °C temperature led to the formation of green crystals suitable for a single crystal X-ray diffraction study. Yield 13.4%. The molecular structure of (**3**) is shown in (Figures 2.9, 2.10). X-ray data is attached in the appendix.

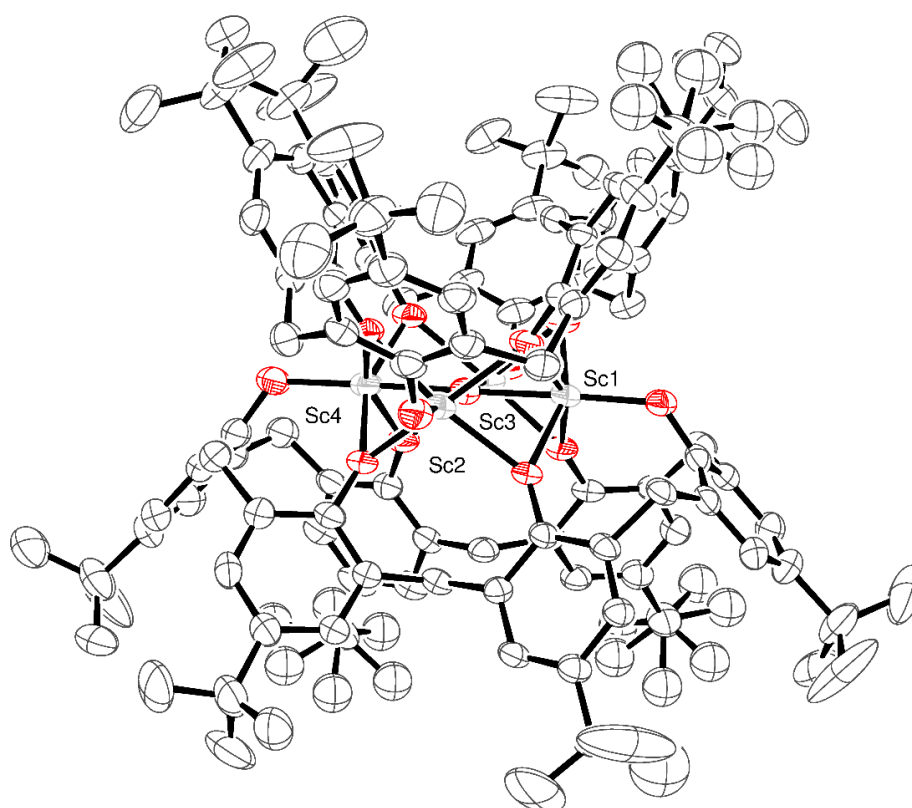


**Figure 2.9.** View of molecular structure of complex (**3**). The hydrogen atoms are removed for clarification. Selected bond lengths (Å) and angles (°): O1-Sc1 1.939(4), O2-Sc1 2.112(4), O6-Sc1 2.151(4), O7-Sc1 2.158(4), O11-Sc1 2.157(4), O13-Sc1 2.084(4), Sc1-Sc3 2.9376(15), Sc1-Sc2 2.9452(15); O1-Sc1-O13 177.49(15), O1-Sc1-O2 98.60(15), O13-Sc1-O2 78.99(14), O1-Sc1-O6 100.89(15), O2-Sc1-O6 97.37(14), O1-Sc1-Sc3 133.87(12), O13-Sc1-Sc3 44.67(10), O2-Sc1-Sc3 47.58(10), O1-Sc1-Sc2 136.38(12), O13-Sc1-Sc2 44.90(10), O2-Sc1-Sc2 112.79(11), Sc3-Sc1-Sc2 89.55(4).

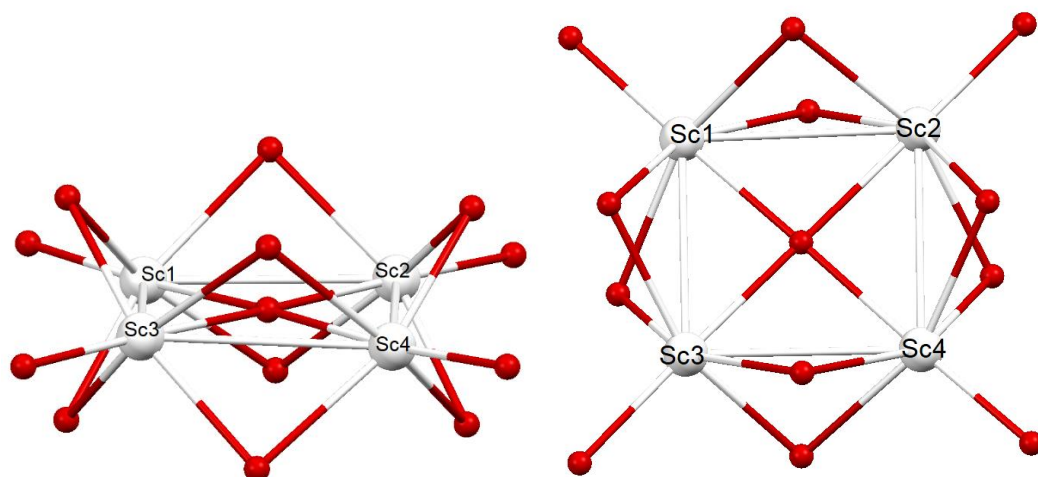


**Figure 2.10.** Core of complex (3). For clarity, only the Sc and O atoms are shown from two different view angles.

There are four Sc ions in a planar square with a central oxygen ion in the same plane. Above and below the plane are two calix[6]arene molecules Bound to the Sc ions. The top and bottom calix[6]arenes are rotated by about 180 degrees to each other.

The source of the sodium in the complex is thought to be impurity from the starting material. I have contacted the manufacturer of the starting material (Sigma Aldrich) and they confirmed the use of sodium in the starting material to make the scandium(III) isopropoxide, which we believe to be the reason behind its presence. The solvents used for the reaction and crystallization are dried using sodium metal and benzophenone which could be the source of the sodium in the crystal.

2.3.2. In an attempt to make a scandium calix[6]arene complex by the introduction of *p-tert*-butylcalix[6]arene with *n*-butyl lithium solution (1.6 M in hexanes) and scandium(III) chloride in THF, the reaction afforded the complex  $[(\text{calix-6})_2\text{Li}_4\text{Cl}(\text{THF})_2\text{BuOH}]\cdot\text{MeCN}$  (**4**). Recrystallization from a saturated acetonitrile solution on prolonged standing at room temperature led to the formation of pale yellow crystals suitable for a single crystal X-ray diffraction study. Yield 8.6%. The molecular structure of (**4**) is shown in (Figures 2.11, 2.12). X-ray data is attached in the appendix.

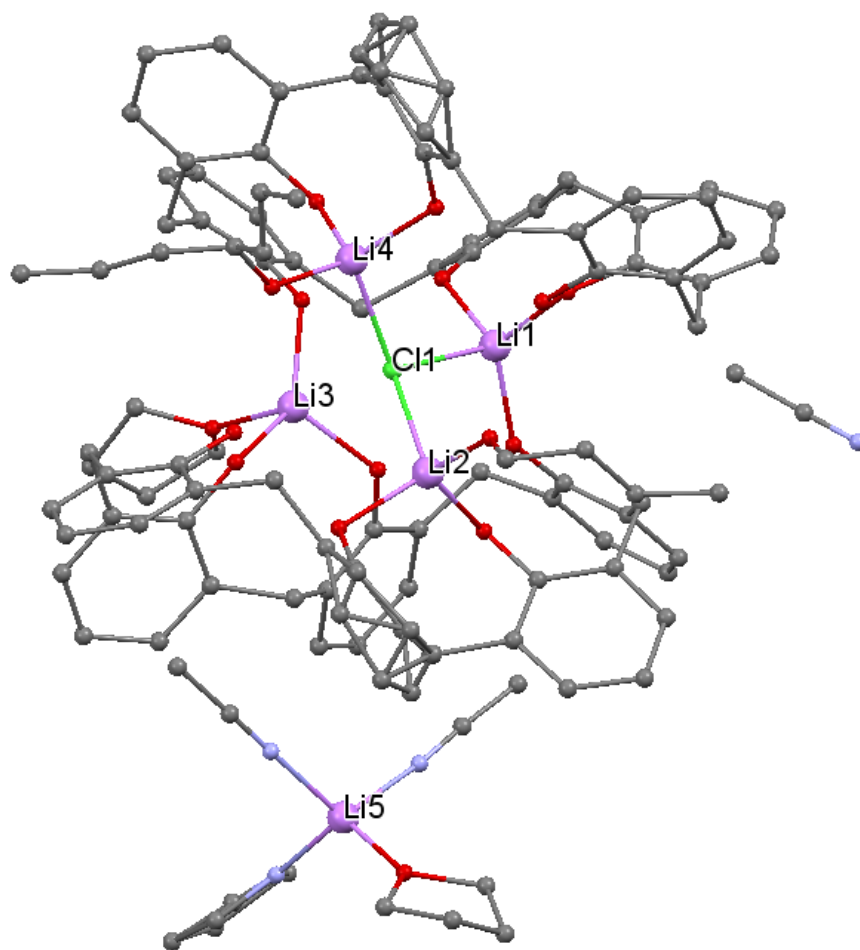


**Figure 2.11.** View of molecular structure of complex (**4**). The hydrogen atoms and *t*-butyl groups of the calix[6]arenes are removed for clarification

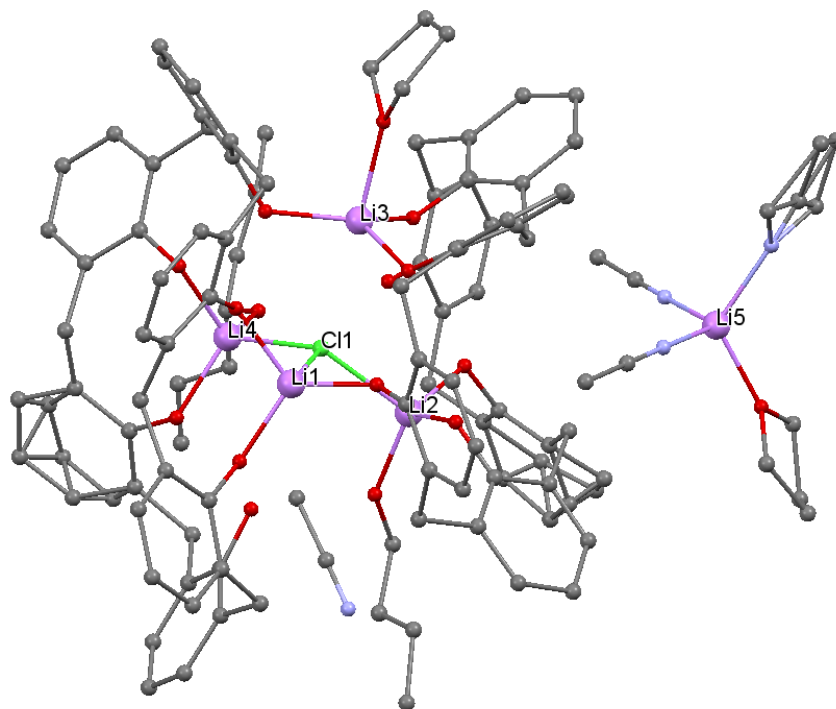


**Figure 2.12.** Alternative view of complex **(4)**. Hydrogen atoms and *t*-butyl groups of the calix[6]arenes are removed for clarification. Selected bond lengths (Å) and angles (°): Cl1-Li2 2.277(8), Cl1-Li4 2.289(8), Cl1-Li1 2.352(7), Cl1-Li3 2.816(8), Li5-N2 2.008(12), Li5-N1 2.012(12), Li5-N3 2.041(13), Li2-Cl1-Li4 124.3(3), Li2-Cl1-Li1 104.7(3), Li4-Cl1-Li1 109.1(3), Li2-Cl1-Li3 112.4(3), Li4-Cl1-Li3 107.5(3), Li1-Cl1-Li3 94.6(2).

The structure is complicated. With disorder in the ligands, two calix[6]arene ligands are binding by their phenolic edges as follows. The Cl atom is central and binding to it three out of the four lithium atoms (Li1, Li2 and Li4). Those three lithium atoms replaced the hydrogen in 5 phenolic groups from the 1st calix[6]arene and 3 from the 2nd calix[6]arene. Li3 also is binding the two calixarenes by replacing one hydrogen from first calix[6]arene phenolic group and 3 hydrogens from 2nd calix[6]arene phenolic groups. Further, there is one molecule of THF and two of butanol also bound to the lithium ions. In addition to this unit, there is a lithium ion with four ligands: (on average 2xMeCN, 1xTHF, and then the last site is 64% MeCN and 36%) and there is one further molecule of MeCN within the structure.

## 2.4. *p*-tert-butylcalix[8]arene chemistry

2.4.1. Interaction of *p*-tert-butylcalix[8]arene with scandium(III) triflate and triethylamine in dimethyl sulfoxide and acetone afforded the complex  $[\text{Sc}(\text{tBuCalix}[8]\text{areneH}_5)(\text{DMSO})_3] \cdot \frac{1}{2}\text{DMSO} \cdot 4\frac{1}{2}\text{MeCN}$ . **(5)**. Recrystallization from acetonitrile on prolonged standing at room temperature led to the formation of yellow crystals suitable for a single crystal X-ray diffraction study. Yield 10.5%. The molecular structure of **(5)** is shown in **(Figures 2.13, 2.14)**. X-ray data is attached in the appendix.

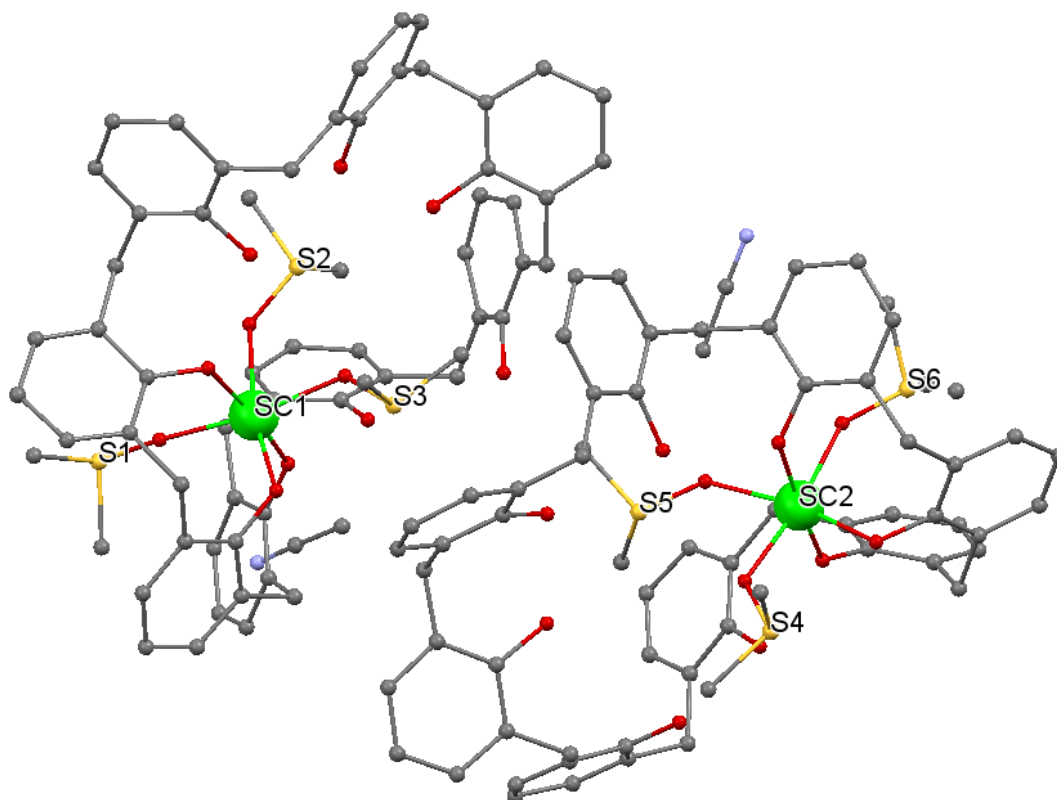
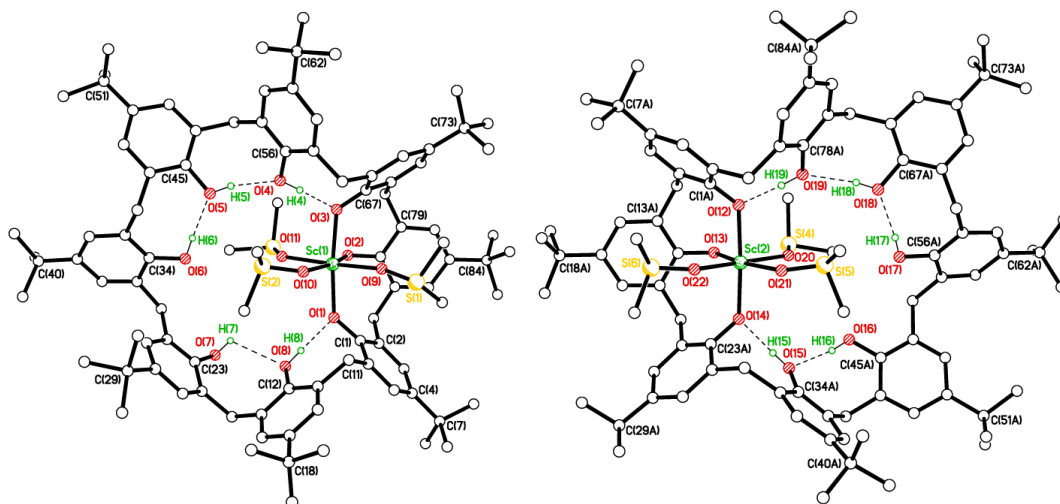


**Figure 2.13.** View of molecular structure of complex **(5)**. The hydrogen atoms and the *t*-butyl groups of calix[8]arene are removed for clarification. Selected bond lengths (Å) and angles (°): Sc1-O1 2.071(3), Sc1-O2 1.997(3), Sc1-O3 2.115(3), Sc1-O9 2.092(3), Sc1-O10 2.176(3), Sc1-O11 2.113(3); Sc1-O1-C1-C2 -79.2(5), Sc1-O11-S3-C93 173.0(3), Sc1-O1-C1-C6 102.3(4), Sc1-O11-S3-C94 -82.5(3), Sc1-O3-C67-C72 74.8(5), Sc1-O3-C67-C68 -106.6(4), Sc1-O2-C78-C83 90.7(4), Sc1-O2-C78-C79 -89.5(4), Sc1-O9-S1-C89 74.8(8), Sc1-O9-S1-C90 178.2(8), Sc1-O10-S2-C92 -149.2(3), Sc1-O10-S2-C91 107.5(3).



Platon squeeze finds 9 voids of which 5 are significant. One lies on a centre of symmetry and is large; the other 4 are related in pairs by symmetry. 376 electrons recovered. This corresponds to 2 DMSO with 2 x 42 electrons, plus 12 x MeCN with 22 electrons each, approx. per unit cell.

The solvent molecules of crystallisation are located in clefts close to or between complexes. There are no significant interactions between complex molecules.

## 2.5. Conclusion

In conclusion, we treated *p-tert*-butylcalix[4]arene with two equivalents of scandium(III) isopropoxide to give the complex (calix-4-H<sub>2</sub>)<sub>6</sub>Sc<sub>9</sub>(OH)<sub>8</sub>(MeCN)<sub>4</sub>·11MeCN (**1**) and with one equivalent of scandium(III) isopropoxide to give the complex [Sc<sub>4</sub>O(calix-4)<sub>4</sub>]·12C<sub>6</sub>H<sub>5</sub>CH<sub>3</sub> (**2**). Furthermore, we treated *p-tert*-butylcalix[6]arene with two equivalents of scandium(III) isopropoxide to give the complex [Sc<sub>4</sub>O(calix-6)<sub>2</sub>]C<sub>8</sub>H<sub>12</sub>N<sub>4</sub>Na<sub>0.5</sub>(C<sub>6</sub>H<sub>9</sub>N<sub>3</sub>Na)·6MeCN (**3**). *p-tert*-butylcalix[6]arene was also treated with scandium(III) chloride after it has been lithiated to give the complex [(calix-6)<sub>2</sub>Li<sub>4</sub>Cl(THF)<sub>2</sub>BuOH].MeCN (**4**). Finally, we treated *p-tert*-butylcalix[8]arene with scandium(III) triflate in the presence of triethylamine and dimethyl sulfoxide to give the complex [Sc(*t*BuCalix[8]areneH<sub>5</sub>)(DMSO)<sub>3</sub>]·½DMSO·4½MeCN (**5**). We discussed the crystallographic structure of these five complexes and some further characterization is in the following experimental section. The Sc-O bond lengths (Å) of complexes (**1**, **2**, **3** and **5**) were in the range (1.932-2.432), which fall in the range of reported similar complexes (Å)(1.912-2.535).<sup>95,99</sup>

## **Chapter 3**

### **Experiment Section**

### 3.1. General Consideration

All reactions were done under an atmosphere of dry nitrogen using Schlenk and cannula techniques or in a glove box filled with nitrogen gas. Hexane, ethanol, methanol, toluene, tetrahydrofuran and acetonitrile were refluxed over sodium. Dichloromethane was refluxed over calcium hydride. Diethylether was dried over sodium benzophenone. All solvents were distilled under nitrogen and degassed before use. <sup>1</sup>H NMR spectra were recorded at room temperature on a Bruker Advance DPX-300 spectrometer or Gemini 300 NMR spectrometer at 300 MHz or a Varian VXR 400 S spectrometer at 400 MHz. The <sup>1</sup>H NMR spectra were calibrated against the residual protio impurity of the deuterated solvent. IR spectra were recorded on a Nicolet Avatar 360 FT IR spectrometer. Elemental analyses were performed at the Department of Chemistry at the University of Hull by the elemental analysis service.

### 3.2. Synthesis of $(\text{calix-4-H}_2)_6\text{Sc}_9(\text{OH})_8(\text{MeCN})_4 \cdot 11\text{MeCN}$ (1).

30 ml of toluene was added to a Schlenk containing *p-tert*-butylcalix[4]arene (0.57 mmol, 0.37 g) and scandium(III) isopropoxide (1.13 mmol, 0.25 g). After refluxing for 24h, the volatiles were removed under reduced pressure, and the residue was extracted into hot acetonitrile (30 ml). Prolonged standing (3-4 days) at room temperature afforded colourless crystals. Yield 7.9 %.

### 3.3. Synthesis of $[\text{Sc}_4\text{O}(\text{calix-4})_4] \cdot 12\text{C}_6\text{H}_5\text{CH}_3$ (2).

30 ml of toluene was added to a Schlenk containing *p-tert*-butylcalix[4]arene (0.57 mmol, 0.37 g) and scandium(III) isopropoxide (1.13 mmol, 0.25 g). After refluxing for 24h, the volatiles were removed under reduced pressure, and the residue was extracted into hot toluene (30 ml) and acetonitrile (30 ml). Prolonged standing (3-4 days) at room temperature afforded colourless crystals. Yield 20.2 %. Calculated values for  $(\text{C}_{176}\text{H}_{208}\text{O}_{17}\text{Sc}_4) \cdot 10(\text{C}_6\text{H}_5\text{CH}_3)8(\text{CH}_3\text{CN})$  C, 78.21; H, 7.76; N, 2.79%. Found: C, 78.10; H, 8.56; N, 2.29%. MALDI-MS:  $m/z = 2776$ .  $^1\text{H}$  NMR (400 MHz,  $(\text{CD}_3)_2\text{CO}$ )  $\delta$ : 6.31-7.07 (m, 32H, ArylH), 2.38-5.72 (m, 32H, ArCHHAr), 1.01-1.32 (m, 144H,  $\text{CH}_3$ ).

### 3.4. Synthesis of [Sc<sub>4</sub>O(calix-

#### 6)<sub>2</sub>]C<sub>8</sub>H<sub>12</sub>N<sub>4</sub>Na0.5(C<sub>6</sub>H<sub>9</sub>N<sub>3</sub>Na)·6MeCN (3).

30 ml of toluene was added to a Schlenk containing *p-tert*-butylcalix[6]arene (0.57 mmol, 0.55 g) and scandium(III) isopropoxide (1.13 mmol, 0.25 g). After refluxing for 24h, the volatiles were removed under reduced pressure, and the residue was extracted into hot acetonitrile (20 ml). the solution afforded green crystals after leaving at a temperature of 0 °C for 5 days. Yield 13.4 %. MALDI-MS: m/z = 2129.

### 3.5. Synthesis of [(calix-6)<sub>2</sub>Li<sub>4</sub>Cl(THF)<sub>2</sub>BuOH]·MeCN (4).

*p-tert*-butylcalix[6]arene (1.65 mmol, 1.6 g) and 25 ml of THF were mixed in a 100 mL flask. *n*-Butyl lithium solution (1.6 M in hexanes) (9.6 mmol, 6 mL) was added dropwise to the mixture. After stirring for 24 h at room temperature, scandium(III) chloride (3.3 mmol, 0.5 g) was introduced to the reaction. After stirring for 24 h, the solvent was distilled under reduced pressure, and 25 mL of acetonitrile was introduced to recrystallize. Prolonged standing (3-4 days) at room temperature afforded pale yellow crystals. Yield 8.6 %.

### 3.6. Synthesis of

#### **[Sc(*t*BuCalix[8]areneH<sub>5</sub>)(DMSO)<sub>3</sub>] $\cdot$ 1/2DMSO $\cdot$ 4 1/2MeCN. (5).**

In a Schlenk, a solution of Sc(OTf)<sub>3</sub> (0.36 mmol, 0.17 g) in 5 mL dimethyl sulfoxide was added to a solution of *p-tert*-butylcalix[8]arene (0.32 mmol, 0.42 g) and triethylamine (1.45 mmol, 0.15 g) in 20 ml of acetone. After stirring for 5 minutes, the solution was filtered and left to form crystals at room temperature. Yield 10.5 %. MALDI-MS:  $m/z = 1671$

([Sc(*t*BuCalix[8]areneH<sub>5</sub>)(DMSO)<sub>3</sub>]+DMSO+1/2MeCN). <sup>1</sup>H NMR (400 MHz, C<sub>6</sub>D<sub>6</sub>)  $\delta$ : 9.70-14.7 (m, 5H, OH), 7.30-7.42 (m, 16H, ArylH), 3.23-5.28 (m, 16H, ArCHHAr), 1.45-1.88 (m, 18H, CH<sub>3</sub>-S-CH<sub>3</sub>), 1.08-1.38 (m, 72H, CH<sub>3</sub>). IR (KBr) cm<sup>-1</sup>: 3614 (w), 3280 (m), 2720 (m), 2532 (m), 1747 (w), 1699 (w), 1597 (w), 1568 (w), 1391 (s), 1363 (s), 1290 (s), 1232 (s), 1208 (s), 1121 (m), 1058 (s), 1030 (s), 1010 (s), 959 (s), 909 (m), 878 (m), 814 (m), 800 (m), 773 (m), 754 (m), 743 (m), 734 (m), 705 (w), 698 (w), 669 (w), 665 (w), 638 (m), 599 (w), 572 (w), 518 (m), 496 (w), 467 (m), 456 (m), 437 (m), 415 (m).

## References

1. World Health Organization, <http://www.who.int/news-room/fact-sheets/detail/cancer>, (accessed March 2018).
2. S. Huclier-Markai, R. Kerdjoudj, C. Alliot, A. Bonraisin, N. Michel, F. Haddad and J. Barbet, *Nucl. Med. Biol.*, 2014, **41**, e36-e43.
3. M. Pniok, V. Kubiček, J. Havlíčková, J. Kotek, A. Sabatie-Gogová, J. Plutnar, S. Huclier-Markai and P. Hermann, *Chemistry—A European Journal*, 2014, **20**, 7944-7955.
4. D. E. Reichert, J. S. Lewis and C. J. Anderson, *Coord. Chem. Rev.*, 1999, **184**, 3-66.
5. M. A. Lodge, H. Braess, F. Mahmoud, J. Suh, N. Englar, S. Geysers-Stoops, J. Jenkins, S. L. Bacharach and V. Dilsizian, *The Journal of invasive cardiology*, 2005, **17**, 491-496.
6. A. Rahmim and H. Zaidi, *Nucl. Med. Commun.*, 2008, **29**, 193-207.
7. N. Ferrara, *Recent Prog. Horm. Res.*, 2000, **55**, 15-35; discussion 35-16.
8. J. Folkman, *N. Engl. J. Med.*, 1995, **333**, 1757-1763.
9. G. Nagy, D. Szikra, G. Trencsényi, A. Fekete, I. Garai, A. M. Giani, R. Negri, N. Masciocchi, A. Maiocchi and F. Uggeri, *Angew. Chem.*, 2017, **129**, 2150-2154.
10. M. D. Bartholomä, *Inorg. Chim. Acta*, 2012, **389**, 36-51.
11. V. Carroll, D. W. Demoin, T. J. Hoffman and S. S. Jurisson, *Radiochimica acta*, 2012, **100**, 653-667.
12. C. S. Cutler, H. M. Hennkens, N. Sisay, S. Huclier-Markai and S. S. Jurisson, *Chem. Rev.*, 2012, **113**, 858-883.
13. E. W. Price and C. Orvig, *Chem. Soc. Rev.*, 2014, **43**, 260-290.
14. C. F. Ramogida and C. Orvig, *Chem. Commun.*, 2013, **49**, 4720-4739.
15. T. J. Wadas, E. H. Wong, G. R. Weisman and C. J. Anderson, *Chem. Rev.*, 2010, **110**, 2858-2902.
16. B. M. Zeglis and J. S. Lewis, *Dalton Transactions*, 2011, **40**, 6168-6195.
17. F. Roesch, *Current radiopharmaceuticals*, 2012, **5**, 187-201.
18. R. Hernandez, H. F. Valdovinos, Y. Yang, R. Chakravarty, H. Hong, T. E. Barnhart and W. Cai, *Mol. Pharm.*, 2014, **11**, 2954-2961.
19. K. Kolsky, V. Joshi, L. Mausner and S. Srivastava, *Appl. Radiat. Isot.*, 1998, **49**, 1541-1549.
20. F. Rösch and R. P. Baum, *Dalton transactions*, 2011, **40**, 6104-6111.
21. R. P. Baum and H. R. Kulkarni, *Theranostics*, 2012, **2**, 437.
22. L. Mausner, K. Kolsky, V. Joshi and S. Srivastava, *Appl. Radiat. Isot.*, 1998, **49**, 285-294.
23. B. Bartoś, A. Majkowska, S. Krajewski and A. Bilewicz, *Journal*, 2012, **100**, 457.
24. L. F. Mausner, V. Joshi and K. L. Kolsky, *J. Nucl. Med.*, 1995, Medium: X; Size: pp. 104P.423.
25. M. Połosak, A. Piotrowska, S. Krajewski and A. Bilewicz, *J. Radioanal. Nucl. Chem.*, 2013, **295**, 1867-1872.
26. J. E. Duval and M. H. Kurbatov, *Journal of the American Chemical Society (U.S.)*, 1953, Medium: X; Size: Pages: 2246-2248.

27. S. Krajewski, I. Cydzik, K. Abbas, A. Bulgheroni, F. Simonelli, U. Holzwarth and A. Bilewicz, *Journal*, 2013, **101**, 333.
28. G. W. Severin, J. W. Engle, H. F. Valdovinos, T. E. Barnhart and R. J. Nickles, *Appl. Radiat. Isot.*, 2012, **70**, 1526-1530.
29. I. Ahmad, G. Bonino, G. C. Castagnoli, S. M. Fischer, W. Kutschera and M. Paul, *Phys. Rev. Lett.*, 1998, **80**, 2550-2553.
30. D. V. Filosofov, N. S. Loktionova and F. Rösch, *Journal*, 2010, **98**, 149.
31. M. Mirza and A. Aziz, *Radiochimica Acta*, 1969, **11**, 43-64.
32. D. Schumann, S. Horn and J. Neuhausen, *Annual Report*, 2006, 41.
33. E. Seidl and K. Lieser, *Radiochimica Acta*, 1973, **19**, 196-198.
34. K. Zhernosekov, M. Bunka, A. Hohn, R. Schibli and A. Turler, *J. Labelled Compd. Radiopharm.*, 2011, **54**, S239.
35. S. Krajewski, I. Cydzik, K. Abbas, A. Bulgheroni, F. Simonelli, A. Majkowska-Pilip and A. Bilewicz, *Nucl Med Rev*, 2012, **15**, A22-A46.
36. C. Müller, M. Bunka, J. Reber, C. Fischer, K. Zhernosekov, A. Turler and R. Schibli, *J. Nucl. Med.*, 2013, **54**, 2168-2174.
37. C. Müller, H. Struthers, C. Winiger, K. Zhernosekov and R. Schibli, *J. Nucl. Med.*, 2013, **54**, 124-131.
38. S. Cotton, *Polyhedron*, 1999, **12**, 1691-1715.
39. P. R. Meehan, D. R. Aris and G. R. Willey, *Coord. Chem. Rev.*, 1999, **181**, 121-145.
40. G. A. Melson and R. W. Stotz, *Coord. Chem. Rev.*, 1971, **7**, 133-160.
41. M. Pruszyński, A. Majkowska-Pilip, N. S. Loktionova, E. Eppard and F. Roesch, *Appl. Radiat. Isot.*, 2012, **70**, 974-979.
42. E. Koumariou, N. Loktionova, M. Fellner, F. Roesch, O. Thews, D. Pawlak, S. Archimandritis and R. Mikolajczak, *Appl. Radiat. Isot.*, 2012, **70**, 2669-2676.
43. S. Eigner, D. R. B. Vera, M. Fellner, N. S. Loktionova, M. Piel, O. Lebeda, F. Rösch, T. L. Roß and K. E. Henke, *Mol. Imaging Biol.*, 2013, **15**, 79-86.
44. E. Da Silva, A. Lazar and A. Coleman, *J. Drug Deliv. Sci. Technol.*, 2004, **14**, 3-20.
45. A. Baeyer, *Berichte der deutschen chemischen gesellschaft*, 1872, **5**, 1094-1100.
46. L. Lederer, *Journal für Praktische Chemie*, 1894, **50**, 223-226.
47. O. Manasse, *Berichte der deutschen chemischen Gesellschaft*, 1894, **27**, 2409-2413.
48. A. Zinke, E. Ziegler, E. Martinowitz, H. Pichelmayer, M. Tomio, H. Wittmann-Zinke and S. Zwanziger, *Berichte der Deutschen Chemischen Gesellschaft [Abteilung] B: Abhandlungen*, 1944, 264-272.
49. J. Cornforth, P. A. Hart, G. Nicholls, R. Rees and J. Stock, *Br. J. Pharmacol. Chemother.*, 1955, **10**, 73-86.
50. C. Gutsche, *UK: Royal Society of Chemistry*, 1989.
51. A. Arduini and A. Casnati, *Journal*, 1996.
52. T. I., S. A. and B. V., in *Calixarenes 2001*, Springer, Dordrecht, 2001, pp. 26-53.
53. W. Verboom, S. Datta, Z. Asfari, S. Harkema and D. N. Reinhoudt, *The Journal of Organic Chemistry*, 1992, **57**, 5394-5398.
54. C. Jaime, J. De Mendoza, P. Prados, P. M. Nieto and C. Sanchez, *The Journal of Organic Chemistry*, 1991, **56**, 3372-3376.

55. J. O. Magrans, J. de Mendoza, M. Pons and P. Prados, *The Journal of Organic Chemistry*, 1997, **62**, 4518-4520.
56. A. Arduini, A. Pochini, S. Raverberi and R. Ungaro, *J. Chem. Soc., Chem. Commun.*, 1984.
57. C. D. Gutsche and I. Alam, *Tetrahedron*, 1988, **44**, 4689-4694.
58. F. Arnaud-Neu, S. Fanni, L. Guerra, W. McGregor, K. Ziat, M.-J. Schwing-Weill, G. Barrett, M. A. McKerverey, D. Marrs and E. M. Seward, *Journal of the Chemical Society, Perkin Transactions 2*, 1995.
59. R. Roy and J. Mi Kim, *Amphiphilep-tert-Butylcalix[4]arengerüste mit Kohlenhydratkopfgruppen-haltigen Dendronen*, 1999.
60. S. Shinkai, S. Mori, H. Koreishi, T. Tsubaki and O. Manabe, *J. Am. Chem. Soc.*, 1986, **108**, 2409-2416.
61. F. Arnaud-Neu, E. M. Collins, M. Deasy, G. Ferguson, S. J. Harris, B. Kaitner, A. J. Lough, M. A. McKerverey and E. Marques, *J. Am. Chem. Soc.*, 1989, **111**, 8681-8691.
62. M. A. McKerverey, E. M. Seward, G. Ferguson, B. Ruhl and S. J. Harris, *J. Chem. Soc., Chem. Commun.*, 1985.
63. P. F., M. M., S. P. and C. A. W., *First step in the study of the cellular toxicity of the calixarene*, Abstracts, ISSC XI, Fukuoka, 2000.
64. P. Shahgaldian, E. Da Silva and A. W. Coleman, *J. Incl. Phenom. Macrocycl. Chem.*, 2003, **46**, 175-177.
65. E. Memişoğlu, A. Bochot, M. Özalp, M. Şen, D. Duchêne and A. A. Hincal, *Pharm. Res.*, 2003, **20**, 117-125.
66. E. Da Silva, P. Shahgaldian and A. W. Coleman, *Int. J. Pharm.*, 2004, **273**, 57-62.
67. A. Lazar, E. Da Silva, A. Navaza, C. Barbey and A. W. Coleman, *Chem. Commun.*, 2004, 2162-2163.
68. E. D. Silva, D. Ficheux and A. Coleman, *J. Incl. Phenom. Macrocycl. Chem.*, 2005, **52**, 201-206.
69. A. Motornaya, L. Alimbarova, E. Shokova and V. Kovalev, *Pharm. Chem. J.*, 2006, **40**, 68-72.
70. W. Davies, R. Grunert, R. Haff, J. McGahen, E. Neumayer, M. Paulshock, J. Watts, T. Wood, E. Hermann and C. Hoffmann, *Science*, 1964, **144**, 862-863.
71. L. K. Tsou, G. E. Dutschman, E. A. Gullen, M. Telpoukhovskaia, Y.-C. Cheng and A. D. Hamilton, *Bioorg. Med. Chem. Lett.*, 2010, **20**, 2137-2139.
72. A. Casnati, M. Fabbi, N. Pelizzi, A. Pochini, F. Sansone, R. Unguro, E. Di Modugno and G. Tarzia, *Bioorg. Med. Chem. Lett.*, 1996, **6**, 2699-2704.
73. R. Lamartine, M. Tsukada, D. Wilson and A. Shirata, *Comptes Rendus Chimie*, 2002, **5**, 163-169.
74. F. Nasuhi Pur and K. A. Dilmaghani, *J. Coord. Chem.*, 2014, **67**, 440-448.
75. K. Hulíková, V. Grobárová, R. Křivohlavá and A. Fišerová, *Folia Microbiol. (Praha)*, 2010, **55**, 528-532.
76. S. Cherenok, A. Vovk, I. Muravyova, A. Shivanyuk, V. Kukhar, J. Lipkowski and V. Kalchenko, *Org. Lett.*, 2006, **8**, 549-552.
77. G. M. Consoli, G. Granata, E. Galante, I. Di Silvestro, L. Salafia and C. Geraci, *Tetrahedron*, 2007, **63**, 10758-10763.

78. R. P. Dings, X. Chen, D. M. Hellebrekers, L. I. van Eijk, Y. Zhang, T. R. Hoye, A. W. Griffioen and K. H. Mayo, *J. Natl. Cancer Inst.*, 2006, **98**, 932-936.
79. R. P. Dings, J. I. Levine, S. G. Brown, L. Astorgues-Xerri, J. R. MacDonald, T. R. Hoye, E. Raymond and K. H. Mayo, *Invest. New Drugs*, 2013, **31**, 1142-1150.
80. R. Kamada, W. Yoshino, T. Nomura, Y. Chuman, T. Imagawa, T. Suzuki and K. Sakaguchi, *Bioorg. Med. Chem. Lett.*, 2010, **20**, 4412-4415.
81. K. J. Pelizzaro-Rocha, M. B. de Jesus, R. R. Ruela-de-Sousa, C. V. Nakamura, F. S. Reis, A. de Fatima and C. V. Ferreira-Halder, *Biochimica et Biophysica Acta (BBA)-Molecular Cell Research*, 2013, **1833**, 2856-2865.
82. S. Viola, S. Merlo, G. M. Consoli, F. Drago, C. Geraci and M. A. Sortino, *Pharmacology*, 2010, **86**, 182-188.
83. C. Geraci, G. M. Consoli, G. Granata, E. Galante, A. Palmigiano, M. Pappalardo, S. D. Di Puma and A. Spadaro, *Bioconjugate Chem.*, 2013, **24**, 1710-1720.
84. K. J. van Bommel, W. Verboom, R. Hulst, H. Kooijman, A. L. Spek and D. N. Reinhoudt, *Inorg. Chem.*, 2000, **39**, 4099-4106.
85. M. H. Grote Gansey, A. S. de Haan, E. S. Bos, W. Verboom and D. N. Reinhoudt, *Bioconjugate Chem.*, 1999, **10**, 613-623.
86. C. Redshaw, X. Liu, S. Zhan, D. L. Hughes, H. Baillie-Johnson, M. R. Elsegood and S. H. Dale, *Eur. J. Inorg. Chem.*, 2008, **2008**, 2698-2712.
87. C. Redshaw, M. R. Elsegood, J. A. Wright, H. Baillie-Johnson, T. Yamato, S. De Giovanni and A. Mueller, *Chem. Commun.*, 2012, **48**, 1129-1131.
88. J. Kowalewski, D. Kruk and G. Parigi, 2005.
89. D. T. Schühle, J. Schatz, S. Laurent, L. Vander Elst, R. N. Muller, M. C. Stuart and J. A. Peters, *Chemistry—A European Journal*, 2009, **15**, 3290-3296.
90. E. M. Georgiev and D. M. Roundhill, *Inorg. Chim. Acta*, 1997, **258**, 93-96.
91. J. Bryant, L. Henry, A. T. Yordanov, J. J. Linnoila, M. W. Brechbiel and J. A. Frank, *Angew. Chem. Int. Ed.*, 2000, **39**, 1641-1643.
92. S. Aime, A. Barge, M. Botta, A. Casnati, M. Fragai, C. Luchinat and R. Ungaro, *Angew. Chem.*, 2001, **113**, 4873-4875.
93. D. T. Schühle, M. Polášek, I. Lukeš, T. Chauvin, E. Tóth, J. Schatz, U. Hanefeld, M. C. Stuart and J. A. Peters, *Dalton Transactions*, 2010, **39**, 185-191.
94. F. Arnaud-Neu, *Chem. Soc. Rev.*, 1994, **23**, 235-241.
95. C. E. Daitch, P. D. Hampton and E. N. Duesler, *Inorg. Chem.*, 1995, **34**, 5641-5645.
96. Y. Masuda, Y. Zhang, C. Yan and B. Li, *J. Alloys Compd.*, 1998, **275**, 872-876.
97. H. R. Webb, M. J. Hardie and C. L. Raston, *Chemistry—A European Journal*, 2001, **7**, 3616-3620.
98. P. Gou, W. Zhu and Z. Shen, *Science in China Series B: Chemistry*, 2007, **50**, 648-653.
99. F. Estler, E. Herdtweck and R. Anwander, *J. Chem. Soc., Dalton Trans.*, 2002, 3088-3089.

## Appendix

### Crystallographic data for complexes 1, 2 and 3

Identification code	1	2	3
Chemical formula	C <sub>282</sub> H <sub>338</sub> N <sub>10</sub> O <sub>32</sub> Sc <sub>9</sub>	C <sub>204</sub> H <sub>240</sub> O <sub>17</sub> Sc <sub>4</sub>	C <sub>152</sub> H <sub>186</sub> N <sub>10</sub> Na <sub>2</sub> O <sub>13</sub> Sc <sub>4</sub>
Formula weight	4784.24	3143.79	2586.92
Temperature/ K	100(2)	100(2)	100(2)
Wavelength/ Å	0.71075	1.54184	0.71075
Crystal system	Monoclinic	Tetragonal	Monoclinic
Space group	C 2/c	P 4 <sub>2</sub> /n	P 2 <sub>1</sub> /n
Unit cell dimensions			
a/ Å	37.2622(14)	24.45960(10)	16.9405(5)
b/ Å	21.2546(9)	24.45960(10)	31.8951(7)
c/ Å	37.6585(17)	18.34320(10)	30.8200(10)
$\alpha$ / °	90	90	90
$\beta$ / °	106.414(4)	90	101.037(3)
$\gamma$ / °	90	90	90
V/ Å <sup>3</sup>	28610(2)	10974.22(11)	16344.6(8)
Z	8	2	4
Calculated density/ Mg/m <sup>3</sup>	1.111	0.951	1.051
Absorption coefficient/ mm <sup>-1</sup>	0.262	1.415	0.219
F(000)	10180	3368	5512
Crystal size/ mm <sup>3</sup>	0.150 x 0.050 x 0.020	0.200 x 0.050 x 0.040	0.120 x 0.100 x 0.050
Theta range for data collection/ °	1.696 to 25.027	2.555 to 68.234	1.808 to 25.683
Index ranges	-44 ≤ h ≤ 44, - 25 ≤ k ≤ 25, -44 ≤ l ≤ 44	-29 ≤ h ≤ 25, -29 ≤ k ≤ 28, -21 ≤ l ≤ 20	-20 ≤ h ≤ 20, -38 ≤ k ≤ 38, -37 ≤ l ≤ 37
Reflections collected	115121	50463	169806
Independent reflections	25275 [R(int) = 0.0636]	10008 [R(int) = 0.0365]	31037 [R(int) = 0.0863]
Completeness to theta = 25.027°	100.0 %	99.6 %	100.0 %
Absorption correction	Semi-empirical from equivalents	Semi-empirical from equivalents	Semi-empirical from equivalents
Max. and min. transmission	1.00000 and 0.29373	1.0000 and 0.66766	1.000 and 0.68903
Refinement method	Full-matrix least- squares on F <sup>2</sup>	Full-matrix least- squares on F <sup>2</sup>	Full-matrix least- squares on F <sup>2</sup>
Data / restraints / parameters	25275 / 1225 / 1420	10008 / 11 / 457	31037 / 36 / 1547
Goodness-of-fit on F <sup>2</sup>	1.044	1.052	1.027
Final R indices [I > 2σ(I)]	R1 = 0.0825, wR2 = 0.2054	R1 = 0.0823, wR2 = 0.2409	R1 = 0.1132, wR2 = 0.3050
R indices (all data)	R1 = 0.1086, wR2 = 0.2201	R1 = 0.0945, wR2 = 0.2535	R1 = 0.1696, wR2 = 0.3523
Extinction coefficient	n/a	n/a	n/a
Largest diff. peak and hole/ e.Å <sup>-3</sup>	2.674 and -0.694	0.963 and -0.572	1.417 and -0.629

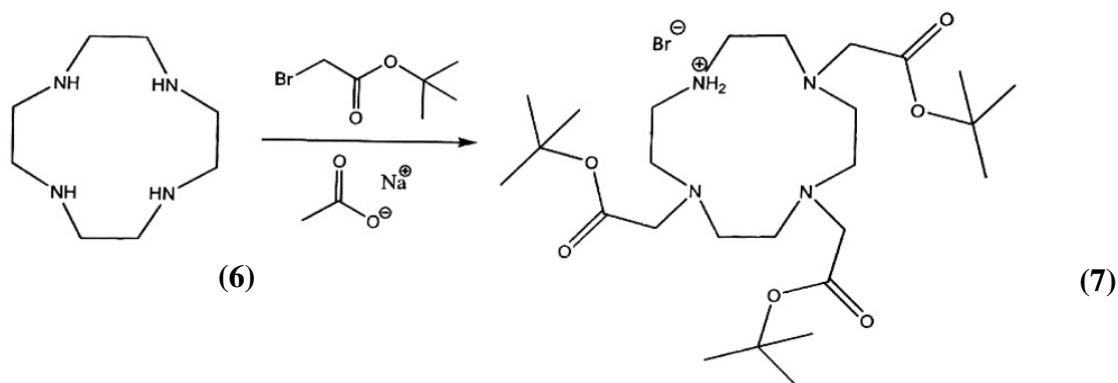
## Crystallographic data for complexes **4** and **5**

Identification code	4	5
Chemical formula	C <sub>156.72</sub> H <sub>200</sub> Cl Li <sub>5</sub> N <sub>4</sub> O <sub>16</sub>	C <sub>94</sub> H <sub>127</sub> O <sub>11</sub> S <sub>3</sub> Sc · 0.5(C <sub>2</sub> H <sub>6</sub> OS) · 4.5(C <sub>2</sub> H <sub>3</sub> N)
Formula weight	2465.98	1797.89
Temperature/ K	100(2)	100
Wavelength/ Å	0.71075	1.54184
Crystal system	Monoclinic	Triclinic
Space group	P 2/c	P <sup>-</sup> 1
Unit cell dimensions		
a/ Å	33.1077(10)	16.6936 (2)
b/ Å	15.7015(4)	18.2801 (3)
c/ Å	33.0469(10)	37.5436 (6)
α/ °	90	101.9761 (13)
β/ °	115.129(4)	90.0656 (13)
γ/ °	90	110.8224 (13)
V/ Å <sup>3</sup>	15553.2(9)	10440.3 (3)
Z	4	4
Calculated density/ Mg/m <sup>3</sup>	1.053	1.144
Absorption coefficient/ mm <sup>-1</sup>	0.083	1.71
F(000)	5313	3872
Crystal size/ mm <sup>3</sup>	0.14 x 0.12 x 0.06	0.20 x 0.02 x 0.02
Theta range for data collection/ °	1.911 to 25.682	2.7 to 63.6
Index ranges	-40 ≤ h ≤ 40, -19 ≤ k ≤ 19, -40 ≤ l ≤ 40	h = -18 → 18, k = -20 → 20, l = -41 → 41
Reflections collected	192441	149975
Independent reflections	29536 [R(int) = 0.1042]	29958 [R(int) = 0.122]
Completeness to theta = 25.027°	99.9 %	
Absorption correction		Multi-scan. CrysAlisPro 1.171.39.34b (Rigaku Oxford Diffraction, 2017) Empirical absorption correction using spherical harmonics, implemented in SCALE3 ABSPACK scaling algorithm.
Max. and min. transmission		0.549, 1.000
Refinement method	Full-matrix least-squares on F <sup>2</sup>	
Data / restraints / parameters	29536 / 16 / 1586	29958 / 1331 / 2323
Goodness-of-fit on F <sup>2</sup>	1.040	
Final R indices [I > 2σ(I)]	R1 = 0.1221, wR2 = 0.3114	R1 = 0.076, wR2 = 0.235
R indices (all data)	R1 = 0.1667, wR2 = 0.3481	
Extinction coefficient	n/a	n/a
Largest diff. peak and hole/ e.Å <sup>-3</sup>	1.374 and -1.766	0.68 and -0.46

The following three ligands were prepared to be used in the scandium coordination chemistry. However, the attempts made to bind to scandium were not successful.

### 1. Synthesis of 1,4,7-tris(*tert*-butoxycarbonylmethyl)-1,4,7,10-tetraazacyclododecane Hydrobromide

The method used was as reported by Jagadish *et al.*<sup>100</sup>



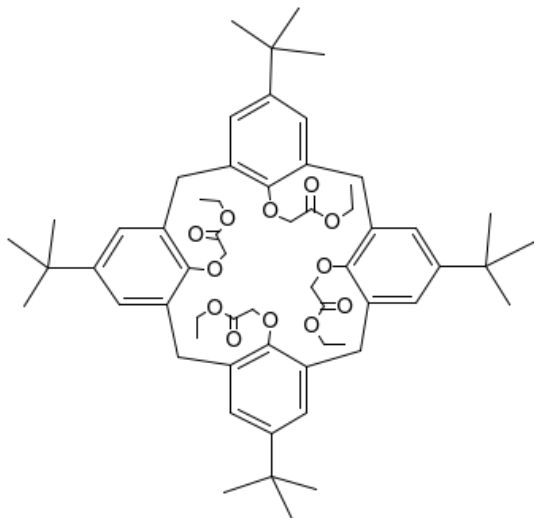
Yield: 39.5 %.

Calculated: C, 52.43; H, 8.63; N, 9.41%;

Found: C, 52.22; H, 8.85; N, 9.37%.

<sup>1</sup>H NMR as reported in the literature.<sup>100</sup>

## 2. 4-*tert*-Butylcalix[4]arenetetraacetic acid tetraethyl ester:



The modified method of Chang *et al.* was employed.<sup>101</sup> The difference is that there is no need for column chromatography and it can be replaced by recrystallization with methanol.

The tetra ester calix[4]arene was prepared as follows:

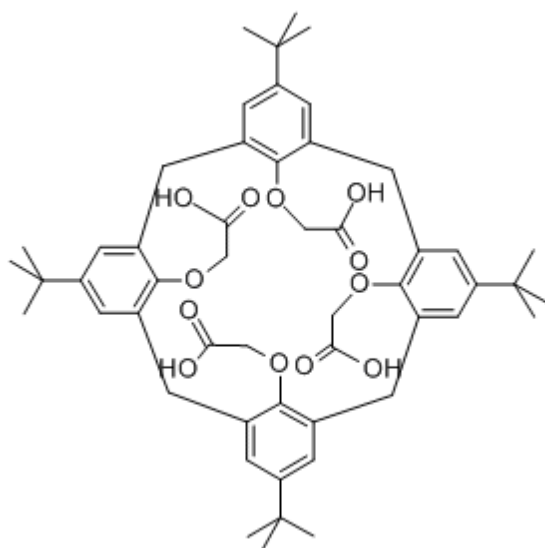
A calix[4]arene (6 mmol, 3.9 g) was suspended in dry DMF (30 ml) in a flask equipped with a CaCl<sub>2</sub> drying tube and was then treated with 60% NaH (72 mmol, 2.94 g). Ethyl bromoacetate (96 mmol, 10.6 ml) was added and the mixture was stirred at 85 °C for 24 hours. The solvent was evaporated under reduced pressure, and the residue was dissolved in 200 ml CH<sub>2</sub>Cl<sub>2</sub> and moved to the separation funnel. It was washed once with 100 ml 10% HCl and washed with water twice. The CH<sub>2</sub>Cl<sub>2</sub> solution was then dried over MgSO<sub>4</sub> and filtered. The solvent then was evaporated to give the solid crude product. Instead of the Column chromatography in this step, 200 ml of methanol was added and stirred for 10 minutes. After that, it was left to crystallize at room temperature. Yield: 2.9 g.

Calculated; C, 72.55; H, 8.12%;

Found: C, 72.28; H, 8.32%.

$^1\text{H}$  NMR as reported in the literature.<sup>101</sup>

**3. 4-*tert*-Butylcalix[4]arene tetra acetic acid:**



Made by hydrolysis of the 4-*tert*-Butylcalix[4]arene tetra acetic acid tetraethyl ester using the method reported by Chang *et al.*<sup>101</sup>

Yield 91%.

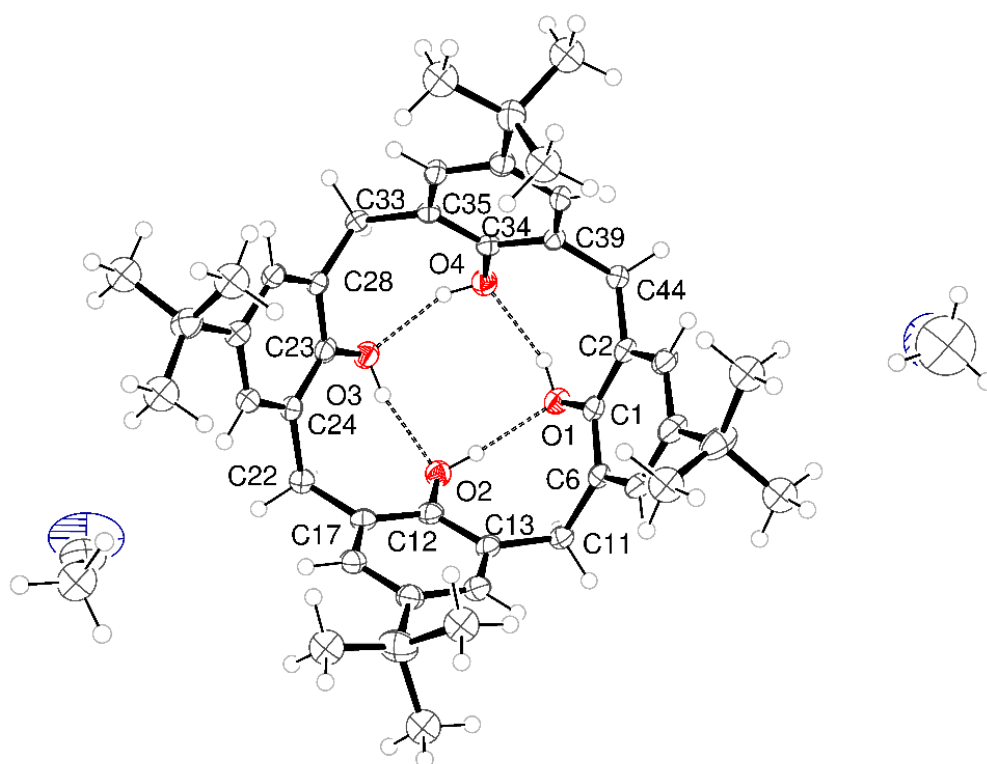
Calculated: C, 70.89; H, 7.32%;

Found: C, 70.64; H, 7.46%.

$^1\text{H}$  NMR as reported in the literature.<sup>101</sup>

On many trials to react the calixarene with scandium, the resulting product is the parent calixarene without scandium. Presumably, the product is very sensitive to hydrolysis. The following crystallographic data is an example

**4-*tert*-butylcalix[4]arene-2MeCN**



## Crystal data and structure refinement for Calix-4.

Empirical formula	C <sub>94</sub> H <sub>121</sub> N <sub>3</sub> O <sub>8</sub>
Formula weight	1420.93
Temperature	100(2) K
Wavelength	1.54184 Å
Crystal system	Orthorhombic
Space group	P n a 21
Unit cell dimensions	a = 26.28380(10) Å      α = 90°. b = 12.59510(10) Å      β = 90°. c = 12.55940(10) Å      γ = 90°.
Volume	4157.75(5) Å <sup>3</sup>
Z	2
Density (calculated)	1.135 Mg/m <sup>3</sup>
Absorption coefficient	0.552 mm <sup>-1</sup>
F(000)	1540
Crystal size	0.243 x 0.166 x 0.061 mm <sup>3</sup>
Theta range for data collection	3.892 to 68.243°.
Index ranges	-31 ≤ h ≤ 31, -15 ≤ k ≤ 15, -
14 ≤ l ≤ 15	
Reflections collected	37412
Independent reflections	6656 [R(int) = 0.0240]
Completeness to theta = 67.684°	99.6 %
Refinement method	Full-matrix least-squares on F <sup>2</sup>
Data / restraints / parameters	6656 / 48 / 448
Goodness-of-fit on F <sup>2</sup>	1.031
Final R indices [I > 2σ(I)]	R1 = 0.0553, wR2 = 0.1546
R indices (all data)	R1 = 0.0566, wR2 = 0.1563
Absolute structure parameter	0.05(6)
Extinction coefficient	n/a
Largest diff. peak and hole	0.374 and -0.478 e.Å <sup>-3</sup>

## Reference

100. Jagadish, B., Brickert-Albrecht, G.L., Nichol, G.S., Mash, E.A. and Raghunand, N., 2011. On the synthesis of 1, 4, 7-tris (*tert*-butoxycarbonylmethyl)-1, 4, 7, 10-tetraazacyclododecane. *Tetrahedron letters*, 52(17), pp.2058-2061.
101. Chang, S.K. and Cho, I., 1986. New metal cation-selective ionophores derived from calixarenes: their syntheses and ion-binding properties. *J. Chem. Soc., Perkin Trans. 1*, pp.211-214.